Supporting Information for

Starburst Triarylamine Donor-based Metal-free Photosensitizers for Photocatalytic Hydrogen Production from Water

Po-Yu Ho,[†,‡,∥] Yi Wang,[†,∥] Sze-Chun Yiu,[†] Wai-Hong Yu,[†] Cheuk-Lam Ho,*[,†,‡] and Shuping Huang*[,§]

[†]Institute of Molecular Functional Materials, Department of Chemistry and Institute of Advanced Materials, Hong Kong Baptist University, Waterloo Road, Kowloon Tong, Hong Kong, P. R. China. E-mail: clamho@hkbu.edu.hk.
[‡]HKBU Institute of Research and Continuing Education, Shenzhen Virtual University Park, Shenzhen, 518057, P. R. China
[§]College of Chemistry, Fuzhou University, Fuzhou, Fujian, 350108, P. R. China. E-mail: huangshp@gmail.com.

Contents

1. Experimental section

Materials and reagents

All chemical reactions were performed under an inert nitrogen atmosphere with the use of a Schlenk line. Glassware was dried in oven prior to use. Commercially available reagents were used without purification. All the reagents for chemical synthesis were purchased from Tokyo Chemical Industry Co., Ltd (TCI), Sigma-Aldrich, Acros Organics or Dieckmann. Solvents were dried by distillation over suitable drying agents. All the reactions were monitored by thin-layer chromatography (TLC) with Merck pre-coated aluminium plates. Products were purified by column chromatography on silica gel (230−400 mesh) purchased from Merck.

Instrumentation

Proton and carbon NMR spectra were measured in $CDCl_3$ or THF-d_8 on a Bruker Ultra-shield 400 MHz FT-NMR spectrometer and tetramethylsilane (TMS) was exploited as an internal standard for calibrating the chemical shift. Matrix-assisted laser desorption ionization time-of-flight (MALDI-TOF) mass spectrometry was performed on an Autoflex Bruker MALDI-TOF system. UV/Vis absorption spectroscopy was performed on a Hewlett Packard 8453 spectrometer in dichloromethane solution at 293 K. The solution emission spectra and lifetimes of the photosensitizers were measured on a Photon Technology International (PTI) Fluorescence QuantaMaster Series QM1 spectrophotometer at 293 K. The decay curves were analysed using a Marquardt-based nonlinear least-squares fitting routine and were shown to follow a single-exponential function in each case according to $I = I_0 + A \exp(-t/\tau)$. Electrochemical

measurements were conducted on a CHI 630C Electrochemical Analyzer/Workstation at a scan rate of 100 mV s^{-1}.

Fabrication and characterization of DSSCs

The procedures for preparation of TiO_2 electrodes and fabrication of the sealed cells for photovoltaic measurements were adapted from that reported by Grätzel and co-workers.[1] A screen-printed double layer of TiO_2 particles was used as the photoelectrode. The area of all the TiO_2 electrodes were 0.28 cm^2. The detailed procedure was referred to a previous work.[2] Then, the photoelectrode was dipped into a 0.2 mM photosensitizer-containing chloroform/ethanol (v/v, 1/1) mixture for 12 hours at room temperature. The counter electrode was prepared according to a previously reported procedure.[2] Finally, the DSSCs were assembled, with the electrolyte solution containing 0.1 M LiI, 0.05 M I_2, 0.6 M 1-butyl-3-methyl imidazolium iodide (BMII) and 0.5 M 4-*tert*-butylpyridine (TBP) in a mixture of acetonitrile and valeronitrile (volume ratio of 1:1).

The photovoltaic measurements employed an AM 1.5 solar simulator equipped with a 300 W xenon lamp (model no. 91160, Oriel). The power of the simulated light was calibrated to 100 mW cm^{-2} using a Newport Oriel PV reference cell system (model 91150 V). *I*−*V* curves were obtained by applying an external bias to the cell and measuring the generated photocurrent with a model 2400 source meter (Keithley Instruments, Inc. USA). The voltage step and delay time of the photocurrent were 10 mV and 40 ms, respectively. The action spectra of the incident monochromatic photo-to-electron conversion efficiency (IPCE) for the solar cells were obtained with a Newport-74125 system (Newport Instruments). The intensity of monochromatic light was

measured with a Si detector (Newport-71640). The electrochemical impedance spectroscopy (EIS) measurements of all the DSSCs were performed using a Zahner IM6e Impedance Analyzer (ZAHNER-Elektrik GmbH & CoKG, Kronach , Germany). The frequency range is from 0.1 Hz to 100 KHz. The magnitude of the alternative signal is 10 mV.

Preparation of platinized TiO_2

For a 0.5 wt-% platinized TiO_2 sample, addition of 40 mL methanol to 1.6 g of titanium(IV) oxide nanopowder (anatase, < 25 nm particle size, 99.7% trace metals basis, Sigma-Aldrich) and 0.1 mL of H_2PtCl_6 aqueous solution (8 wt. %) created slurry which was then subjected to radiation from a 300 W coated Hg lamp (HF300PD, EYE Lighting) under vigorously stirring for 24 hours. The resulting crude product had a grayish colour. Platinized TiO_2 was then retrieved by centrifugation at 3500 rpm for 5 minutes and washed three times with methanol. The obtained material was dried under vacuum at ~ 60 °C in darkness for eight hours.

Adsorption of photosensitizer onto platinized TiO_2

20 mg of the prepared platinized TiO_2 was added to 2.5 mL of 50 μM photosensitizer dichloromethane solution, the mixture was then evenly sonicated for 30 minutes. The solution became colourless gradually while the solid became purple-red in colour. The dye-loaded solid was then retrieved by centrifugation at 3500 rpm for 5 minutes. The supernatant layer solvent was removed carefully using a dropper and the pellet at the bottom was dried under vacuum for

two to three hours in darkness. At the end, the whole dried pellet was directly utilized in the photocatalytic reaction mixture for one photolysis experiment without further characterization.

The dye-loading percentage (DL%) for each PS was estimated by comparing the absorbance value of low-energy absorption peak before and after the dye adsorption (Table 2). All these carboxylate anchor-based PSs attached onto the photocatalyst favourably and almost 100% of the PS was adsorbed. The UV/vis spectra and corresponding images for **S2** in CH_2Cl_2 solution (50 μM) before and after dye attachment are illustrated in Figure S36 as an example in estimating the dye-loading value. The corresponding UV/vis spectra for **S1** and **S3** are shown in Figure S37 and S38, respectively.

Light-driven hydrogen production studies

The photocatalytic reactions were carried out in 5 mL aqueous ascorbic acid (AA, 0.5 M) solution at pH 4.0 with AA serving as the SED (AA is selected in our system, because its relationship between pH value and H_2-evolving activity has been studied in details very recently and the redox chemistry is also well-known.[3]). A 25 mL pear-shaped flask was placed above stirrers at 19 °C and the flask was sealed with rubber septa. The photocatalytic reaction mixture with a stir bar was then purged with a mixture of gas containing argon/methane (80:20 mol%) for 15 minutes. The methane present in the gas mixture was served as an internal standard for GC analysis at the end of each experiment. The reaction mixture was steadily stirred and continuously radiated from the bottom with green (*ca.* 520 nm) light-emitting diodes inside a just-fit container which blocks the stray light from the environment. The light power was measured with a thermal sensor (Model: BIM-7203-0100F) and power meter (Model: BIM-7001;

Hangzhou Brolight Technology Co., Ltd.) and estimated to be ~ 50 mW for each reaction mixture. At the end of the experiment, the headspaces of the flasks were characterized by GC to examine the amount of hydrogen produced. The amounts of hydrogen evolved were determined by using GC (Shimadzu GC-8A with a molecular sieve 5 Å column and TCD detector) at the end of the radiation period and were quantified using a calibration plot of integrated amount of hydrogen relative to the methane (Figure S39). In the course of 48 hours radiation, total six GC samples were taken at different time points (6, 12, 18, 24, 36 and 48 h) from six independent reaction mixtures for photosensitizers **S1**–**S3** (16, 24, 40 and 48 h for **Eosin Y** and blank). The LED radiation is assumed to be monochromatic at emission intensity maximum (520 nm) and the corresponding apparent quantum yield values for each photosensitizer could be estimated according to the equation shown below.

$$\text{AQY}\ (\%) = \frac{\text{rate of } H_2 \text{ production} \times 2}{\text{rate of incident photons}} \times 100\%$$

2. Synthetic procedures of PSs

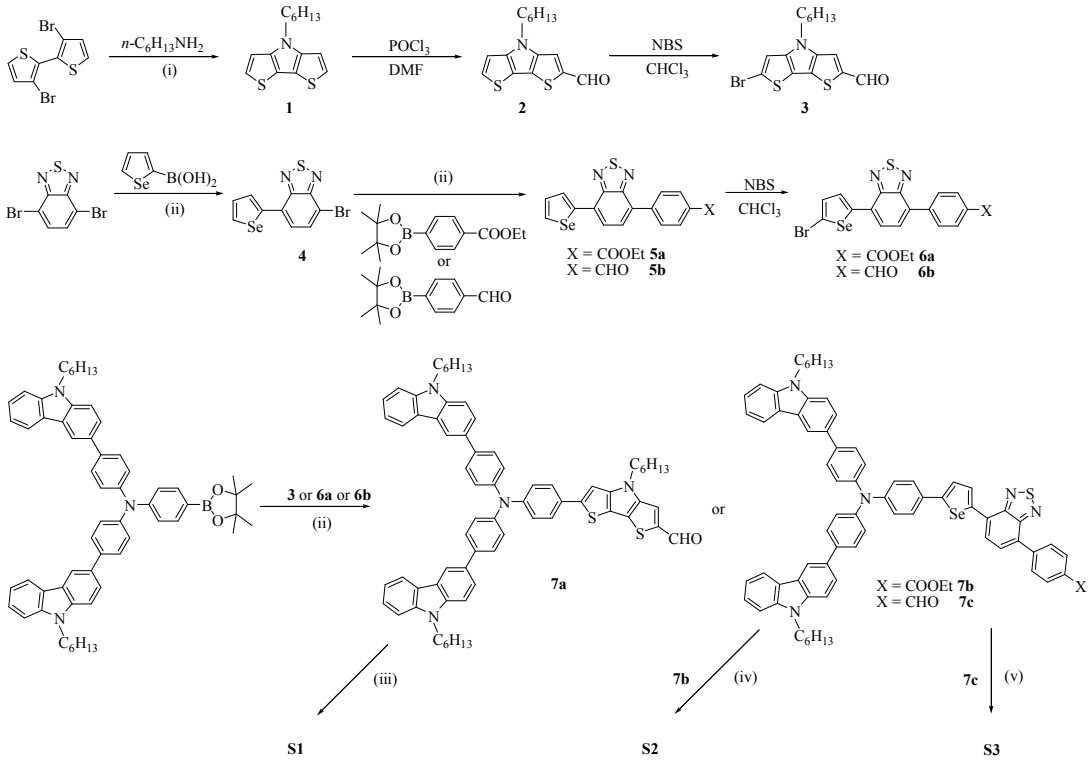

Scheme S1. Synthetic routes for **S1**–**S3**. (i) $[Pd_2(dba)_3]$, $NaOC(CH_3)_3$, toluene, reflux; (ii) $[Pd(PPh_3)_4]$, K_2CO_3, H_2O, tetrahydrofuran, reflux; (iii) $CNCH_2COOH$, piperidine, $CHCl_3$, reflux; (iv) NaOH, H_2O, CH_3OH, tetrahydrofuran, reflux; (v) $CNCH_2COOH$, ammonium acetate, acetic acid, reflux. DMF = dimethylformamide; NBS = *N*-bromosuccinimide.

4-Hexyl-4*H*-dithieno[3,2-b:2',3'-*d*]pyrrole (1). A mixture of 3,3'-dibromo-2,2'-bithiophene (1 g, 3.086 mmol), *n*-hexylamine (0.344 g, 3.395 mmol), $Pd_2(dba)_3$ (71 mg, 0.077 mmol) and sodium *tert*-butoxide (712 mg, 7.406 mmol) in dry toluene (30 mL) was heated to reflux under nitrogen atmosphere overnight. The reaction mixture was poured into water, followed by extraction using ethyl acetate. The organic layer was dried over anhydrous Na_2SO_4 and the solvent was then removed under reduced pressure. The residue was purified by column chromatography on silica gel using a 1:9 mixture of dichloromethane and hexane as eluent to afford compound **1** (0.675 g, 2.562 mmol) as a white solid. ^{1}H NMR (400 MHz, $CDCl_3$): δ = 7.31 (d, 2H, J = 5.2 Hz, Ar),

7.16 (d, 2H, J = 5.2 Hz, Ar), 4.26 (t, 2H, J = 6.8 Hz, alkyl), 2.02−1.97 (m, 2H, alkyl), 1.54−1.51 (m, 6H, alkyl), 1.19−1.15 (m, 3H, alkyl); ^{13}C NMR (100 MHz, $CDCl_3$): δ = 144.73, 122.37, 114.33, 110.81 (Ar), 46.92, 31.22, 30.06, 26.41, 22.36, 13.95 ppm (alkyl). HRMS (MALDI-TOF, m/z): [M^+] 263.0802; calcd for ($C_{14}H_{17}NS_2$) 263.0802.

4-Hexyl-4*H*-dithieno[3,2-*b*:2',3'-*d*]pyrrole-2-carbaldehyde (2). The Vilsemier Haack reagent was first prepared in a two-necked round-bottom flask containing dry DMF (0.163 g, 2.232 mmol). $POCl_3$ (1.711 g, 11.16 mmol) was then dropwisely added by syringe at 0 ^{o}C. Subsequently, a solution of **1** (0.588 g, 2.232 mmol) in dry dichloromethane (20 mL) was added dropwisely to the prepared Vilsmeier-Haack reagent under a nitrogen atmosphere. The mixture was stirred for 15 minutes at 0 ^{o}C and then heated overnight at 55 ^{o}C. After cooling, the reaction was poured into NaOH(aq) solution slowly in an ice bath with stirring for 30 minutes, then the resulting mixture was extracted with dichloromethane and H_2O. The organic fraction was dried over anhydrous Na_2SO_4. The solvent was then removed under reduced pressure and an orange oil was obtained, which was purified by column chromatography on silica gel with hexane/dichloromethane (1:3, v/v) as the eluent to give **2** as a yellow solid (0.488 g, 1.675 mmol). ^{1}H NMR (400 MHz, $CDCl_3$): δ = 9.86 (s, 1H, CHO), 7.63 (s, 1H, Ar), 7.37 (d, 1H, J = 5.2 Hz, Ar), 7.01 (d, 1H, J = 5.2 Hz, Ar), 4.21 (t, 2H, J = 7.2 Hz, alkyl), 1.91−1.84 (m, 2H, alkyl), 1.34−1.25 (m, 6H, alkyl), 0.88−0.86 (m, 3H, alkyl); ^{13}C NMR (100 MHz, $CDCl_3$): δ = 182.89 (CHO), 149.19, 144.16, 139.86, 128.43, 122.78, 119.94, 114.67, 111.05 (Ar), 47.32, 31.32, 30.18, 26.58, 22.48, 14.02 ppm (alkyl). HRMS (MALDI-TOF, m/z): [M^+] 291.0751; calcd for ($C_{15}H_{17}NOS_2$) 291.0752.

6-Bromo-4-hexyl-4*H*-dithieno[3,2-*b*:2',3'-*d*]pyrrole-2-carbaldehyde (3). NBS (0.298 g, 1.675 mmol) was slowly added to a solution of **2** (0.488 g, 1.675 mmol) in $CHCl_3$ (20 mL) at 0 ^{o}C

under darkness. After the mixture was stirred at room temperature overnight, the reaction was terminated by the addition of water. The reaction mixture was then extracted with dichloromethane and water. The organic extract was dried over anhydrous Na_2SO_4 and the solvent was removed under reduced pressure to yield an orange oil which was purified by column chromatography on silica gel with hexane/dichloromethane (1:1, v/v) as the eluent to give **3** as an orange oil (0.540 g, 1.458 mmol). ^{1}H NMR (400 MHz, $CDCl_3$): δ = 9.82 (s, 1H, CHO), 7.57 (s, 1H, Ar), 7.02 (s, 1H, Ar), 4.11 (t, 2H, J = 7.2 Hz, alkyl), 1.83−1.80 (m, 2H, alkyl), 1.31−1.26 (m, 6H, alkyl), 0.88−0.84 (m, 3H, alkyl); ^{13}C NMR (100 MHz, $CDCl_3$): δ = 182.92 (CHO), 146.58, 143.20, 140.32, 122.65, 119.51, 115.45, 114.83, 114.33 (Ar), 47.57, 31.33, 30.21, 26.61, 22.48, 14.01 ppm (alkyl). HRMS (MALDI-TOF, *m*/*z*): [M^+] 368.9860; calcd for ($C_{15}H_{16}BrNOS_2$) 368.9857.

4-Bromo-7-(selenophen-2-yl)benzo[*c*][1,2,5]thiadiazole (4). A mixture of 4,7-dibromobenzo[*c*][1,2,5]thiadiazole (0.4 g, 1.361 mmol), selenophen-2-ylboronic acid (0.25 g, 1.429 mmol), $Pd(PPh_3)_4$ (79 mg, 0.068 mmol) and 2 M aqueous solution of K_2CO_3 (2 mL) in THF (30 mL) was heated to reflux under nitrogen atmosphere overnight. The reaction mixture was poured into water, followed by extraction using ethyl acetate. The organic layer was dried over anhydrous Na_2SO_4 and the solvent was then removed under reduced pressure. The crude product was primarily purified by a short silica column using a 1:2 mixture of dichloromethane and hexane as eluent, in order to remove the catalytic residue and precursor. The yellow solid obtained after solvent removal was immediately subjected to the next reaction without further purification and characterization. HRMS (MALDI-TOF, *m*/*z*): [M^+] 343.8520; calcd for ($C_{10}H_5BrN_2SSe$) 343.8522.

General synthetic procedures of 5a and 5b

A mixture of compound **4** (132 mg, 0.384 mmol), excess ethyl 4-(4,4,5,5-tetramethyl-1,3,2-dioxaborolan-2-yl)benzoate (0.212 g, 0.768 mmol) for **5a** (or 4-(4,4,5,5-tetramethyl-1,3,2-dioxaborolan-2-yl)benzaldehyde (0.178 g, 0.768 mmol) for **5b**), $Pd(PPh_3)_4$ (22 mg, 0.019 mmol) and 2 M aqueous solution of K_2CO_3 (2 mL) in THF (20 mL) was heated to reflux under nitrogen atmosphere overnight. The reaction mixture was poured into water, followed by extraction using ethyl acetate. The organic layer was dried over anhydrous Na_2SO_4 and the solvent was then removed under reduced pressure. The residue was purified by column chromatography on silica gel using a 2:1 mixture of dichloromethane and hexane as eluent to afford compounds **5a** or **5b** as orange solids.

Compound **5a**: 116 mg (73% yield). ^{1}H NMR (400 MHz, $CDCl_3$): δ = 8.20−8.14 (m, 4H, Ar), 8.02−7.99 (m, 2H, Ar), 7.90 (d, 1H, J = 7.6 Hz, Ar), 7.71 (d, 1H, J = 7.6 Hz, Ar), 7.43 (dd, 1H, J = 5.6, 4 Hz, Ar), 4.42 (q, 2H, J = 7.2 Hz, alkyl), 1.42 (t, 3H, J = 7.2 Hz, alkyl); ^{13}C NMR (100 MHz, $CDCl_3$): δ = 166.33 (−C(O)O−), 153.47, 152.67, 143.79, 141.41, 133.96, 131.22, 130.10, 129.99, 129.76, 128.98, 128.64, 128.55, 124.83 (Ar), 61.05, 14.36 ppm (alkyl). HRMS (MALDI-TOF, m/z): [M^+] 413.9942; calcd for ($C_{19}H_{14}N_2O_2SSe$) 413.9941.

Compound **5b**: 102 mg (72% yield). ^{1}H NMR (400 MHz, $CDCl_3$): δ = 10.10 (s, 1H, CHO), 8.25−8.21 (m, 2H, Ar), 8.16−8.14 (m, 2H, Ar), 8.05−8.03 (m, 2H, Ar), 7.99 (d, 1H, J = 7.6 Hz, Ar), 7.80 (d, 1H, J = 7.2 Hz, Ar), 7.43 (dd, 1H, J = 5.6, 4 Hz, Ar); ^{13}C NMR (100 MHz, $CDCl_3$): δ = 191.83 (CHO), 153.49, 152.76, 143.73, 143.11, 135.77, 134.23, 130.94, 130.20, 129.96, 129.71, 129.47, 128.91, 124.87 ppm (Ar). HRMS (MALDI-TOF, m/z): [M^+] 369.9680; calcd for ($C_{17}H_{10}N_2OSSe$) 369.9679.

General synthetic procedures for 6a and 6b

NBS (1.05 molar equivalents) was slowly added to a solution of **5a** (0.116 g, 0.281 mmol) (or **5b** (0.102 g, 0.275 mmol)) in a mixture of $CHCl_3$ (40 mL) and 10 drops of acetic acid at 0 ^oC under darkness. After the mixture was stirred at room temperature overnight, the reaction was terminated by the addition of water. The reaction mixture was then extracted with chloroform and water. The organic extract was dried over anhydrous Na_2SO_4 and the solvent was removed under reduced pressure to yield an orange solid, which was purified by column chromatography on silica gel with hexane/dichloromethane (1:2, v/v) as the eluent to give **6a** as an orange solid (Compound **6b** was purified by multiple precipitations using a mixture of chloroform and methanol after the removal of extraction solvent).

Compound **6a**: 130 mg (94% yield). ^1H NMR (400 MHz, $CDCl_3$): δ = 8.19 (d, 2H, J = 8 Hz, Ar), 8.02 (d, 2H, J = 8.4 Hz, Ar), 7.91−7.89 (m, 1H, Ar), 7.79−7.73 (m, 2H, Ar), 7.36−7.35 (m, 1H, Ar), 4.42 (m, 2H, alkyl), 1.45−1.41 (m, 3H, alkyl); ^{13}C NMR (100 MHz, $CDCl_3$): δ = 166.33 (−C(O)O−), 153.33, 152.56, 145.14, 141.26, 133.20, 131.56, 130.15, 129.83, 128.99, 128.55, 128.18, 127.42, 123.67, 120.51 (Ar), 61.10, 14.37 ppm (alkyl). HRMS (MALDI-TOF, m/z): [M^+] 491.9045; calcd for ($C_{19}H_{13}BrN_2O_2SSe$) 491.9046.

Compound **6b**: 117 mg (95% yield). ^1H NMR (400 MHz, $CDCl_3$): δ = 10.11 (s, 1H, CHO), 8.17−8.15 (m, 2H, Ar), 8.09−8.04 (m, 2H, Ar), 7.99 (d, 1H, J = 7.6 Hz, Ar), 7.92−7.82 (m, 2H, Ar), 7.40 (d, 1H, J = 4 Hz, Ar); ^{13}C NMR (100 MHz, $CDCl_3$): δ = 191.82 (CHO), 153.34, 152.64, 151.53, 145.07, 142.96, 135.78, 133.30, 130.01, 129.73, 128.91, 128.26, 127.71, 125.53, 123.71 ppm (Ar). HRMS (MALDI-TOF, m/z): [M^+] 447.8784; calcd for ($C_{17}H_9BrN_2OSSe$) 447.8784.

General synthetic procedures for 7a−7c

A mixture of compound **3** (31 mg, 0.084 mmol) (or **6a**: 41 mg, 0.083 mmol or **6b**: 35 mg, 0.078 mmol), 4-(9-hexyl-9*H*-carbazol-3-yl)-*N*-(4-(9-hexyl-9*H*-carbazol-3-yl)phenyl)-*N*-(4-(4,4,5,5-tetramethyl-1,3,2-dioxaborolan-2-yl)phenyl)aniline (1.1 molar equivalents), $Pd(PPh_3)_4$ (0.05 molar equivalents) and 2 M aqueous solution of K_2CO_3 (1 mL) in THF (20 mL) was heated to reflux under nitrogen atmosphere overnight. The reaction mixture was poured into water, followed by extraction using ethyl acetate. The organic layer was dried over anhydrous Na_2SO_4 and the solvent was then removed under reduced pressure. The residue was purified by column chromatography on silica gel using a 1:1 mixture of dichloromethane and hexane as eluent to afford compound **7a** (1:3 mixture of hexane and dichloromethane for **7b**; 1:1 mixture of hexane and ethyl acetate for **7c**).

Compound **7a**: 77 mg (89% yield); dark red oil. ^{1}H NMR (400 MHz, $CDCl_3$): δ = 9.84 (s, 1H, CHO), 8.32 (d, 2H, J = 1.6 Hz, Ar), 8.14 (d, 2H, J = 7.6 Hz ,Ar), 7.73−7.65 (m, 6H, Ar), 7.59−7.55 (m, 3H, Ar), 7.50−7.40 (m, 6H, Ar), 7.32−7.29 (m, 4H, Ar), 7.26−7.22 (m, 4H, Ar), 7.14 (s, 1H, Ar), 4.31 (t, 4H, J = 7.2 Hz, alkyl), 4.20 (t, 2H, J = 7.2 Hz, alkyl), 1.92−1.85 (m, 6H, alkyl), 1.35−1.22 (m, 18H, alkyl), 0.90−0.85 (m, 9H, alkyl); ^{13}C NMR (100 MHz, $CDCl_3$): δ = 182.75 (CHO), 149.79, 148.01, 147.69, 145.71, 143.83, 140.92, 139.85, 139.72, 137.35, 131.62, 128.42, 128.13, 126.64, 125.82, 125.15, 124.87, 123.80, 123.39, 123.23, 122.97, 120.42, 118.90, 118.49, 113.65, 108.96, 108.86, 105.51 (Ar), 47.49, 43.25, 31.63, 31.42, 30.28, 29.02, 27.03, 26.72, 22.59, 22.53, 14.05, 14.04 ppm (alkyl). HRMS (MALDI-TOF, m/z): [M^+] 1032.4837; calcd for ($C_{69}H_{68}N_4OS_2$) 1032.4835.

Compound **7b**: 95 mg (99% yield); dark purple solid. ^{1}H NMR (400 MHz, $CDCl_3$): δ = 8.36 (d, 2H, J = 1.2 Hz, Ar), 8.25−8.16 (m, 4H, Ar), 8.09−8.07 (m, 2H, Ar), 7.97 (d, 1H, J = 7.2 Hz, Ar), 7.79−7.74 (m, 3H, Ar), 7.72−7.70 (m, 4H, Ar), 7.64−7.61 (m, 2H, Ar), 7.56 (d, 1H, J = 4 Hz, Ar), 7.56−7.43 (m, 7H, Ar), 7.36−7.34 (m, 3H, Ar), 7.30−7.23 (m, 5H, Ar), 4.49−4.44 (m, 2H, alkyl), 4.34 (t, 4H, J = 7.2 Hz, alkyl), 1.96−1.89 (m, 4H, alkyl), 1.48−1.45 (m, 3H, alkyl), 1.36−1.26 (m, 12H, alkyl), 0.92−0.89 (m, 6H, alkyl); ^{13}C NMR (100 MHz, $CDCl_3$): δ = 166.45 (−C(O)O−), 153.63, 152.74, 147.77, 145.81, 141.68, 141.61, 140.90, 139.83, 137.19, 131.66, 130.90, 130.11, 129.96, 129.85, 129.17, 129.02, 128.72, 128.10, 127.83, 127.01, 125.78, 125.07, 124.94, 124.87, 124.22, 123.37, 123.25, 122.97, 120.43, 118.88, 118.49, 118.35, 108.94, 108.84 (Ar), 61.10, 43.24, 31.62, 29.02, 27.02, 22.58, 14.40, 14.06 ppm (alkyl). HRMS (MALDI-TOF, m/z): [M^+] 1155.4021; calcd for ($C_{73}H_{65}N_5O_2SSe$) 1155.4024.

Compound **7c**: 78 mg (90% yield); dark purple solid. ^{1}H NMR (400 MHz, $CDCl_3$): δ = 10.08 (s, 1H, Ar), 8.32 (d, 2H, J = 1.6 Hz, Ar), 8.18−8.12 (m, 5H, Ar), 8.02−8.00 (m, 2H, Ar), 7.91 (d, 1H, J = 7.6 Hz, Ar), 7.75−7.65 (m, 7H, Ar), 7.58−7.56 (m, 2H, Ar), 7.51−7.40 (m, 7H, Ar), 7.32−7.30 (m, 4H, Ar), 7.25−7.21 (m, 4H, Ar), 4.30 (t, 4H, J = 7.2 Hz, alkyl), 1.92−1.84 (m, 4H, alkyl), 1.44−1.22 (m, 12H, alkyl), 0.88−0.83 (m, 6H, alkyl); ^{13}C NMR (100 MHz, $CDCl_3$): δ = 191.89 (CHO), 153.94, 153.52, 152.72, 147.82, 145.78, 143.20, 141.50, 140.90, 139.83, 137.21, 135.67, 131.64, 130.36, 130.31, 130.02, 129.98, 129.65, 129.53, 128.98, 128.11, 127.02, 125.79, 125.09, 124.96, 124.87, 124.11, 123.37, 123.34, 122.97, 120.43, 118.89, 118.48, 108.95, 108.85 (Ar), 43.24, 31.62, 29.02, 27.02, 22.59, 14.06 ppm (alkyl). HRMS (MALDI-TOF, m/z): [M^+] 1111.3762; calcd for ($C_{71}H_{61}N_5OSSe$) 1111.3762.

Photosensitizer S1. A mixture of compound **7a** (71 mg, 0.070 mmol) and cyanoacetic acid (18 mg, 0.211 mmol) in chloroform (3 mL) was refluxed in the presence of piperidine (42 mg, 0.491

mmol) overnight under a nitrogen atmosphere. After cooling, the reaction mixture was extracted with $CHCl_3$ and water. The solvent was then removed under reduced pressure and the crude product was purified by column chromatography on silica gel eluting with $CHCl_3$, followed by $CHCl_3$/MeOH (10:1, v/v) to give the desired product **S1** as a dark solid (66 mg, 0.058 mmol). ^{1}H NMR (400 MHz, THF-d_8): δ = 8.43 (d, 2H, J = 1.2 Hz, Ar), 8.37 (s, 1H, −C=CH−), 8.19 (d, 2H, J = 8 Hz ,Ar), 7.96 (s, 1H, Ar), 7.79−7.75 (m, 6H, Ar), 7.71−7.69 (m, 2H, Ar), 7.60−7.58 (m, 2H, Ar), 7.54−7.52 (m, 3H, Ar), 7.47−7.43 (m, 2H, Ar), 7.34−7.32 (m, 4H, Ar), 7.26−7.19 (m, 4H, Ar), 4.44 (t, 4H, J = 7.2 Hz, alkyl), 4.38 (t, 2H, J = 7.2 Hz, alkyl), 1.99−1.90 (m, 6H, alkyl), 1.48−1.32 (m, 18H, alkyl), 0.95−0.90 (m, 9H, alkyl); ^{13}C NMR (100 MHz, THF-d_8): δ = 164.60 (COOH), 151.15, 148.80, 148.68, 147.64, 146.52, 145.28, 141.76, 140.66, 138.25, 133.90, 132.26, 129.52, 128.56, 127.11, 126.25, 125.74, 125.38, 125.23, 124.21, 123.82, 120.83, 120.57, 119.37, 118.80, 117.28, 114.33, 109.66, 109.51, 106.80, 95.30 (Ar), 47.72, 43.44, 32.42, 32.21, 30.85, 29.73, 27.61, 27.31, 23.29, 23.22, 14.16 ppm (alkyl). HRMS (MALDI-TOF, m/z): [M^+] 1099.4895; calcd for ($C_{72}H_{69}N_5O_2S_2$) 1099.4893.

Photosensitizer S2. A mixture of compound **7b** (95 mg, 0.082 mmol), 6 mL 20% NaOH(aq) (w/w) and methanol (15 mL) in tetrahydrofuran (25 mL) was refluxed for two hours under a nitrogen atmosphere. After cooling, the organic solvents were removed under reduced pressure, the reaction mixture was then extracted with $CHCl_3$ and water. The crude product was purified by column chromatography on silica gel eluting with $CHCl_3$ and then $CHCl_3$/MeOH (10:1, v/v) to give the desired product **S2** as a dark solid (75 mg, 0.067 mmol). ^{1}H NMR (400 MHz, THF-d_8): δ = 8.39 (s, 2H, Ar), 8.31 (d, 1H, J = 4 Hz, Ar), 8.20−8.15 (m, 7H, Ar), 7.96 (d, 1H, J = 7.6 Hz, Ar), 7.76−7.72 (m, 6H, Ar), 7.66−7.63 (m, 3H, Ar), 7.57−7.54 (m, 2H, Ar), 7.50−7.48 (m, 2H, Ar), 7.43−7.39 (m, 2H, Ar), 7.30 (d, 4H, J = 8 Hz, Ar), 7.23−7.15 (m, 4H, Ar), 4.40 (t, 4H, J

= 7.2 Hz, alkyl), 1.93−1.86 (m, 4H, alkyl), 1.45−1.29 (m, 12H, alkyl), 0.89−0.86 (m, 6H, alkyl); ^{13}C NMR (100 MHz, THF-d_8): δ = 167.28 (COOH), 154.31, 154.27, 153.48, 148.56, 146.61, 142.27, 141.96, 141.74, 140.64, 138.10, 132.27, 131.38, 131.20, 131.12, 130.73, 130.36, 129.70, 129.59, 129.46, 128.54, 127.44, 126.24, 125.68, 125.55, 125.24, 124.73, 124.19, 123.99, 123.82, 120.84, 119.36, 118.78, 109.66, 109.51 (Ar), 43.43, 32.40, 29.72, 27.59, 23.27, 14.16 ppm (alkyl). HRMS (MALDI-TOF, *m*/*z*): [M$^+$] 1127.3712; calcd for ($C_{71}H_{61}N_5O_2SSe$) 1127.3712.

Photosensitizer S3. A mixture of compound **7c** (78 mg, 0.070 mmol) and cyanoacetic acid (60 mg, 0.700 mmol) in acetic acid (8 mL) was refluxed in the presence of ammonium acetate (25 mg) overnight under a nitrogen atmosphere. After cooling, the reaction mixture was extracted with $CHCl_3$ and water. The solvent was then removed under reduced pressure and the crude product was purified by column chromatography on silica gel eluting with $CHCl_3$ followed by $CHCl_3$/MeOH (10:1, v/v) to give the desired product **S3** as a dark solid (68 mg, 0.058 mmol). ^{1}H NMR (400 MHz, THF-d_8): δ = 8.43 (d, 2H, *J* = 1.6 Hz, Ar), 8.37−8.33 (m, 4H, Ar), 8.26−8.24 (m, 2H, Ar), 8.20−8.16 (m, 3H, Ar), 8.01 (d, 1H, *J* = 7.6 Hz, Ar), 7.79−7.75 (m, 6H, Ar), 7.69−7.65 (m, 3H, Ar), 7.59−7.57 (m, 2H, Ar), 7.54−7.51 (m, 2H, Ar), 7.47−7.43 (m, 2H, Ar), 7.34−7.32 (m, 4H, Ar), 7.26−7.19 (m, 4H, Ar), 4.42 (t, 4H, *J* = 7.2 Hz, alkyl), 1.96−1.89 (m, 4H, alkyl), 1.50−1.29 (m, 12H, alkyl), 0.93−0.89 (m, 6H, alkyl) ; ^{13}C NMR (100 MHz, THF-d_8): δ = 163.87 (COOH), 154.78, 154.43, 153.86, 153.71, 148.82, 146.79, 142.37, 141.94, 140.83, 138.33, 132.53, 132.48, 131.86, 131.27, 131.12, 130.90, 130.46, 130.27, 129.78, 128.74, 127.64, 126.42, 125.89, 125.77, 125.43, 124.89, 124.39, 124.15, 124.02, 121.03, 119.55, 118.98, 116.42, 109.84, 109.69, 104.74 (Ar), 43.63, 32.60, 29.92, 27.80, 23.47, 14.35 ppm (alkyl). HRMS (MALDI-TOF, *m*/*z*): [M$^+$] 1127.3712; calcd for ($C_{71}H_{61}N_5O_2SSe$) 1127.3712. HRMS (MALDI-TOF, *m*/*z*): [M$^+$] 1178.3817; calcd for ($C_{74}H_{62}N_6O_2SSe$) 1178.3820.

3. ^{1}H NMR and ^{13}C NMR spectra

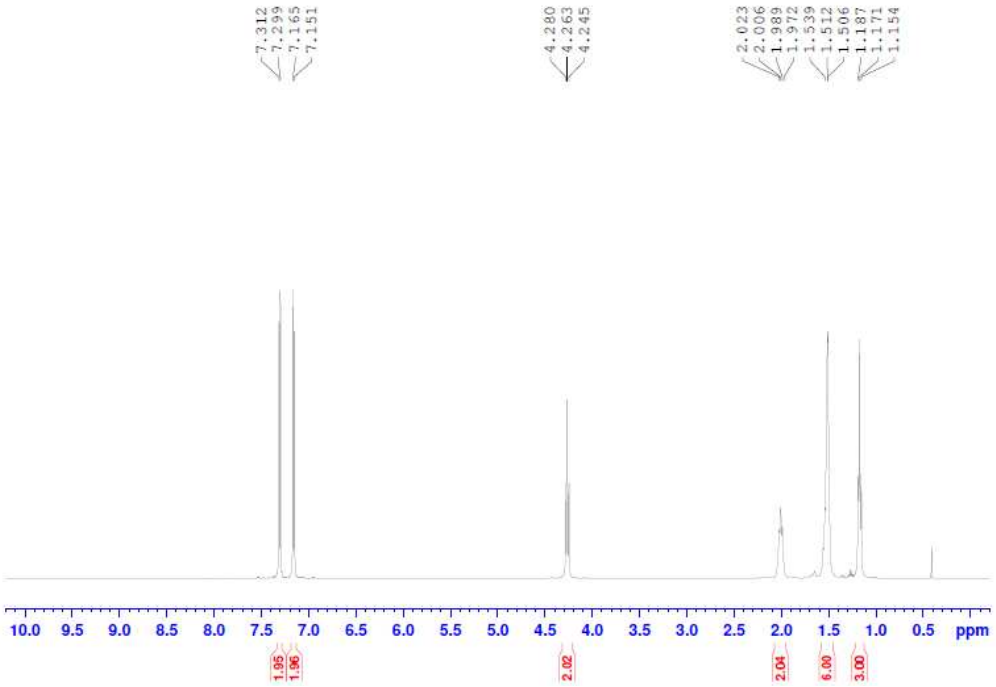

Figure S1. ^{1}H NMR spectrum of **1** in $CDCl_3$.

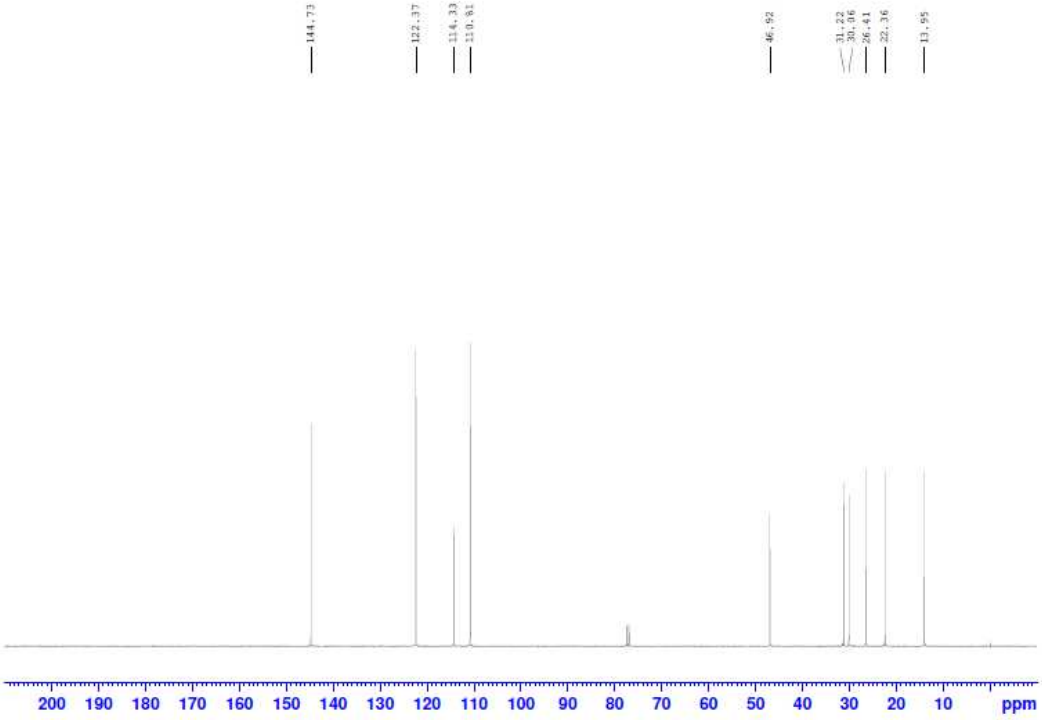

Figure S2. ^{13}C NMR spectrum of **1** in $CDCl_3$.

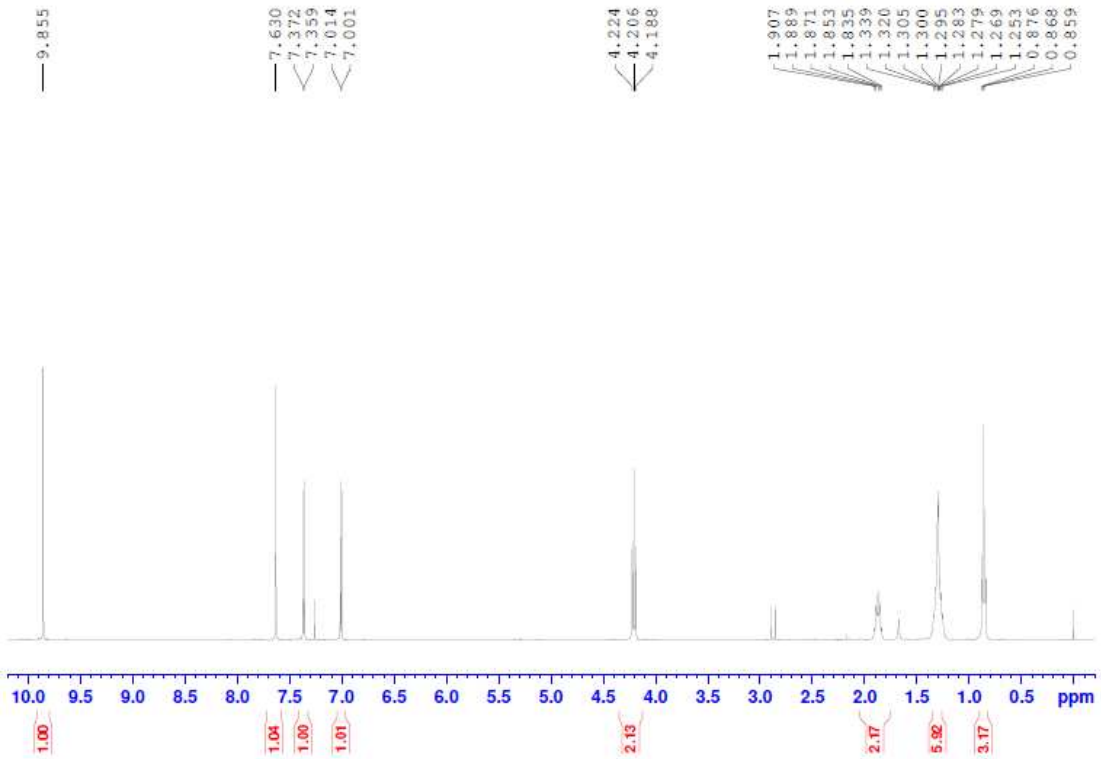

Figure S3. ^{1}H NMR spectrum of **2** in $CDCl_3$.

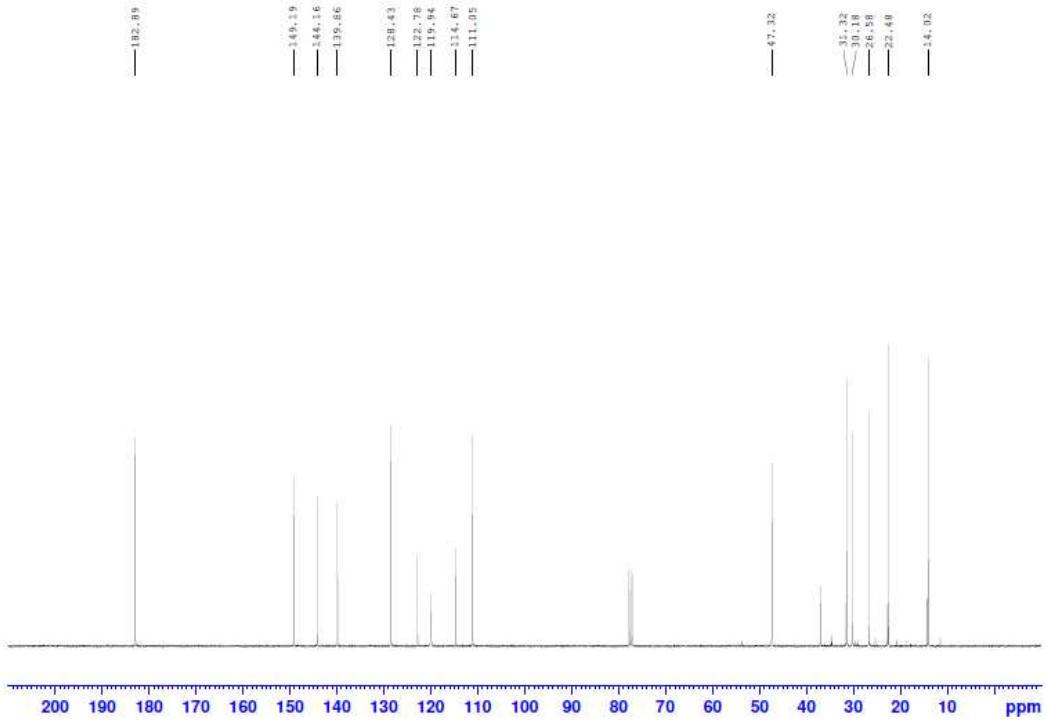

Figure S4. ^{13}C NMR spectrum of **2** in $CDCl_3$.

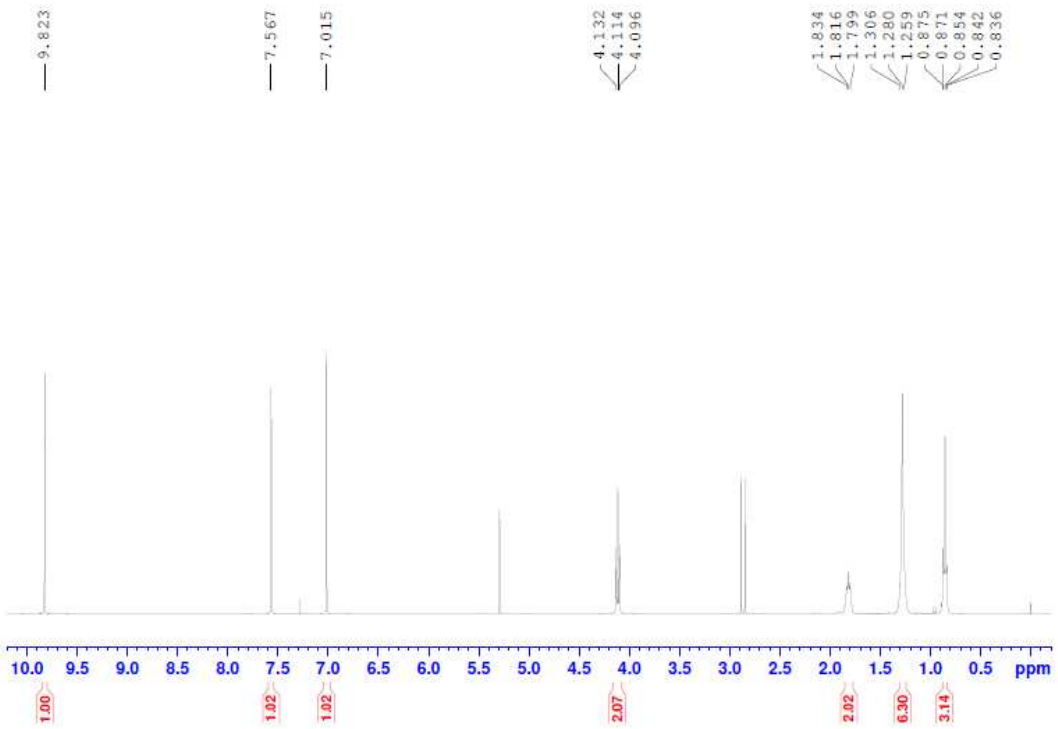

Figure S5. ^{1}H NMR spectrum of **3** in $CDCl_3$.

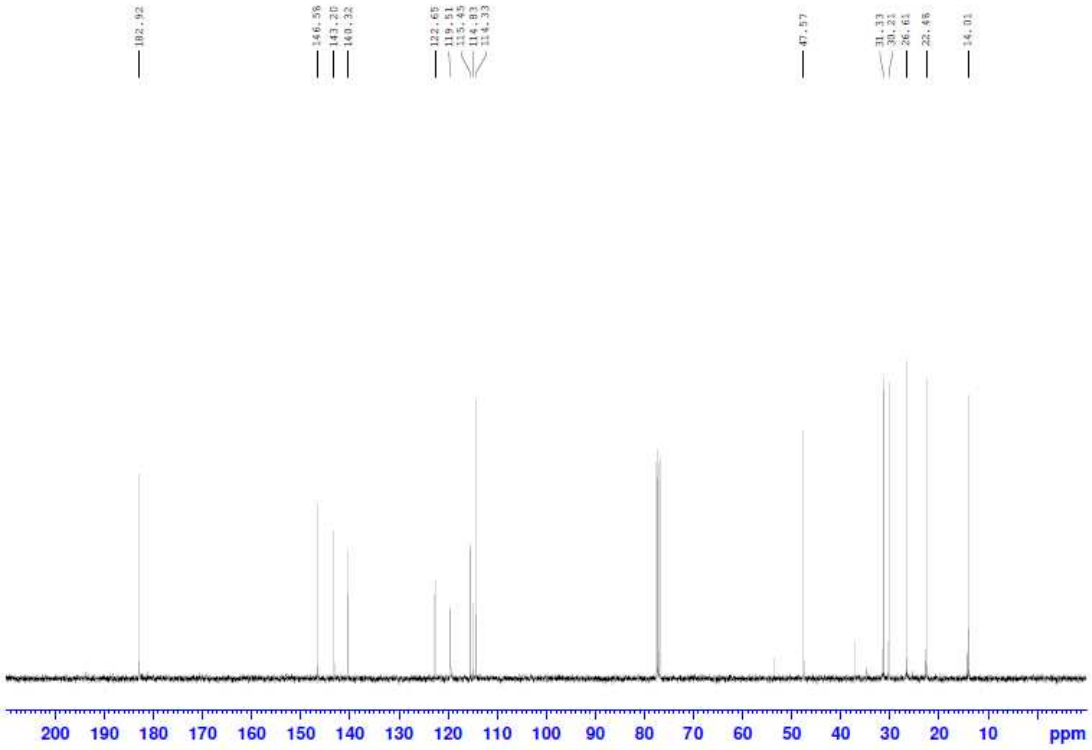

Figure S6. ^{13}C NMR spectrum of **3** in $CDCl_3$.

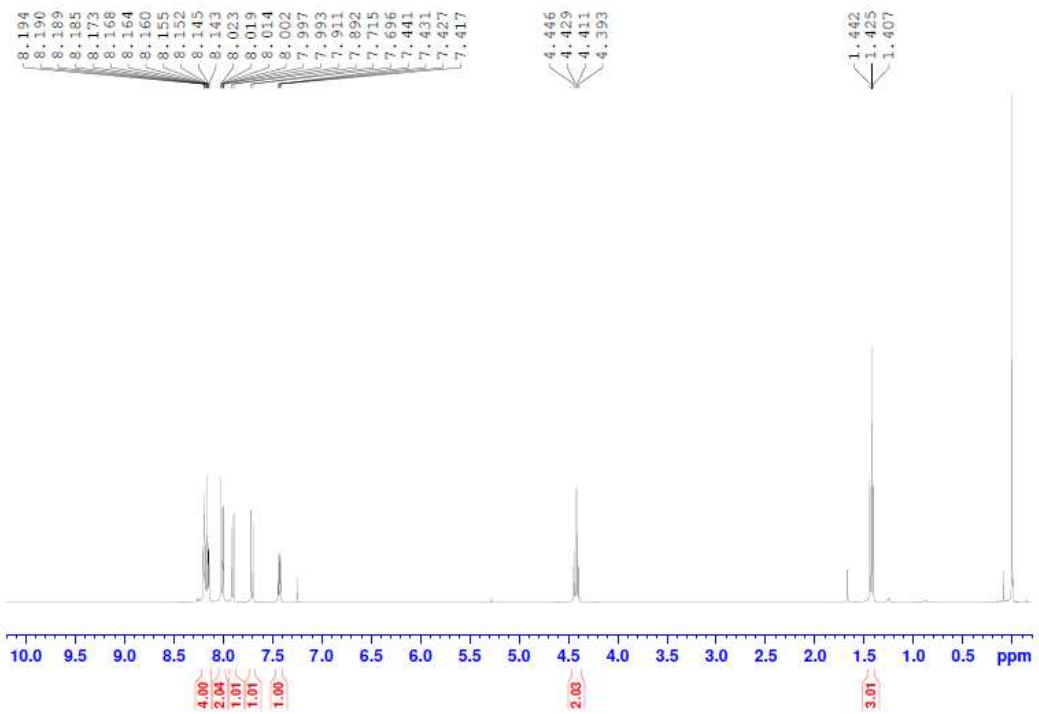

Figure S7. ^{1}H NMR spectrum of **5a** in $CDCl_3$.

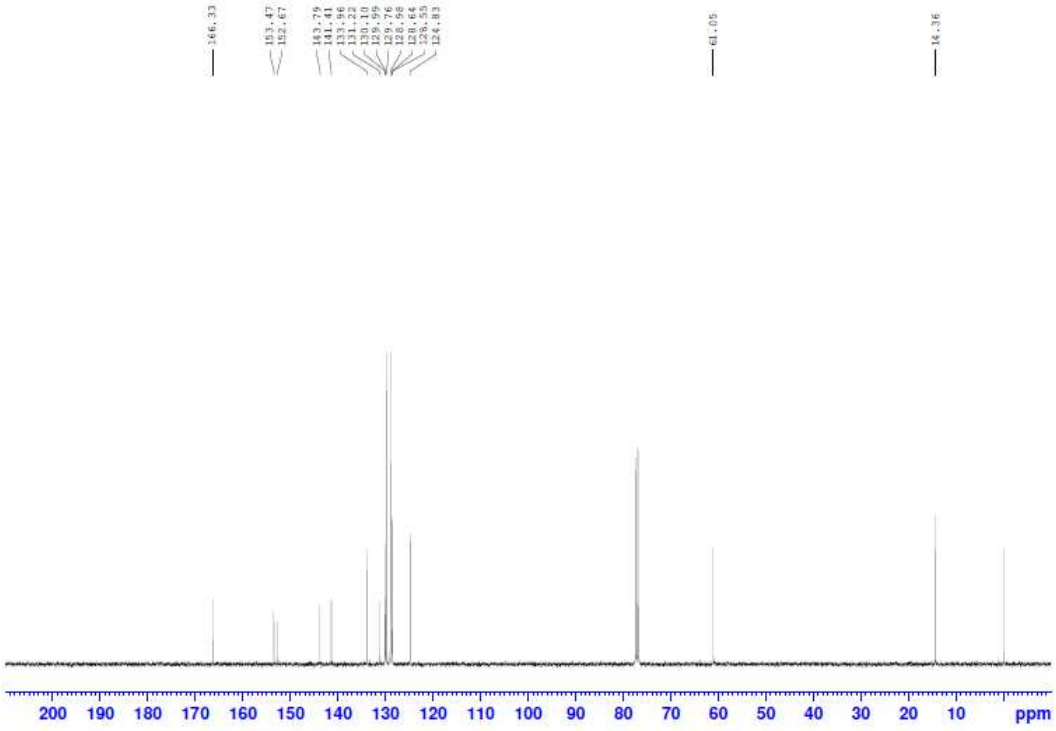

Figure S8. ^{13}C NMR spectrum of **5a** in $CDCl_3$.

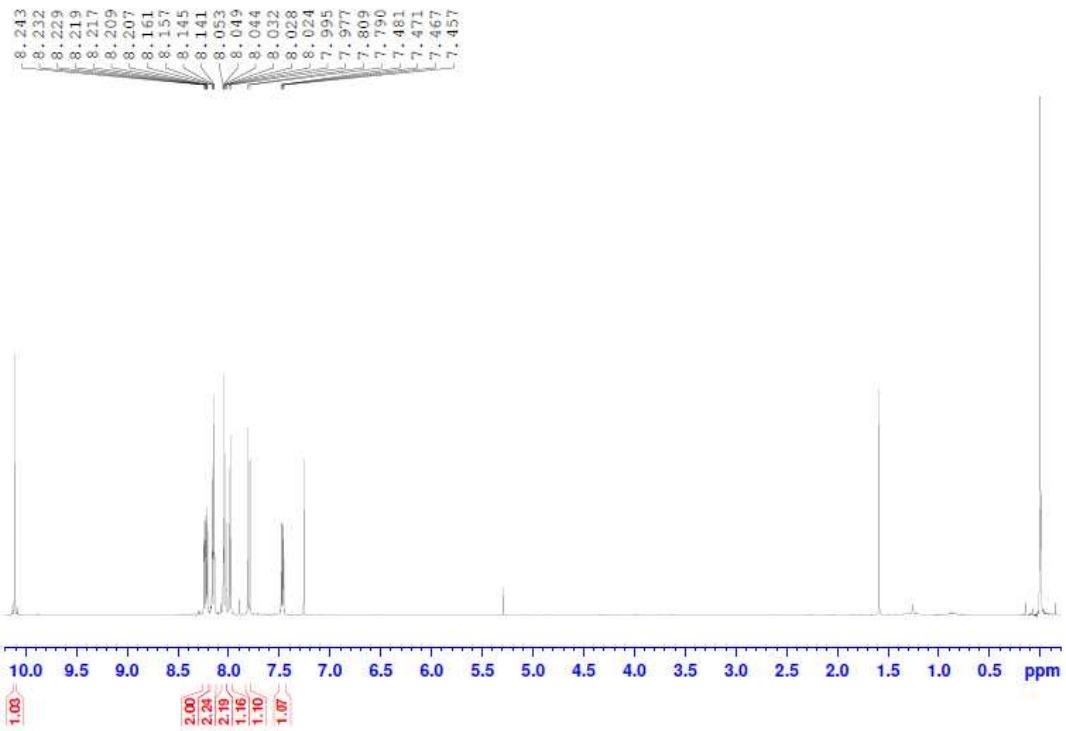

Figure S9. ^{1}H NMR spectrum of **5b** in $CDCl_3$.

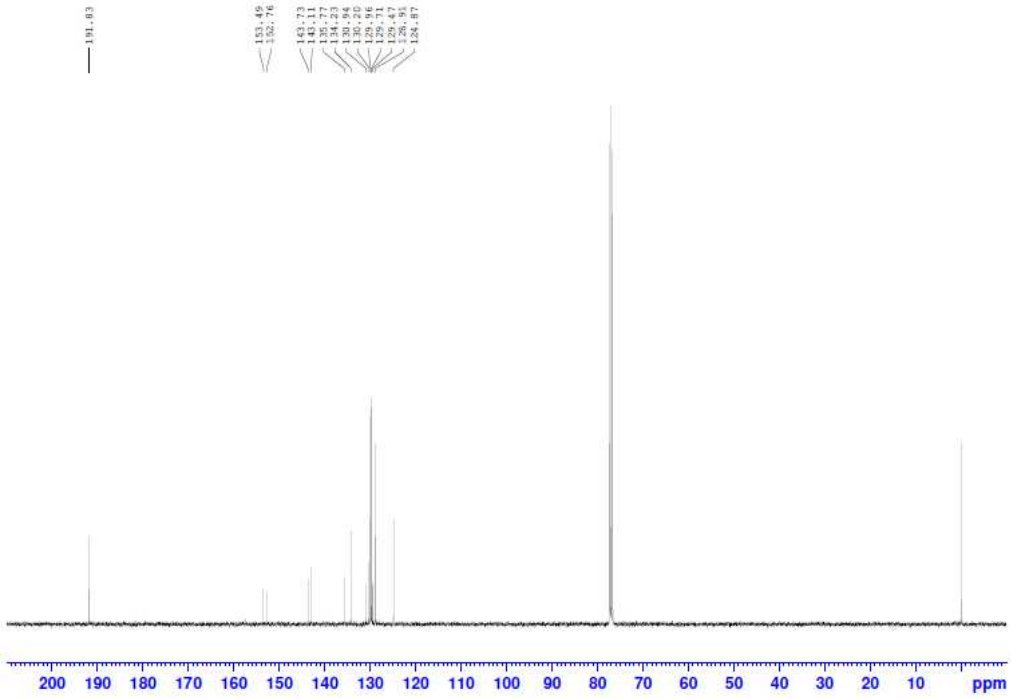

Figure S10. ^{13}C NMR spectrum of **5b** in $CDCl_3$.

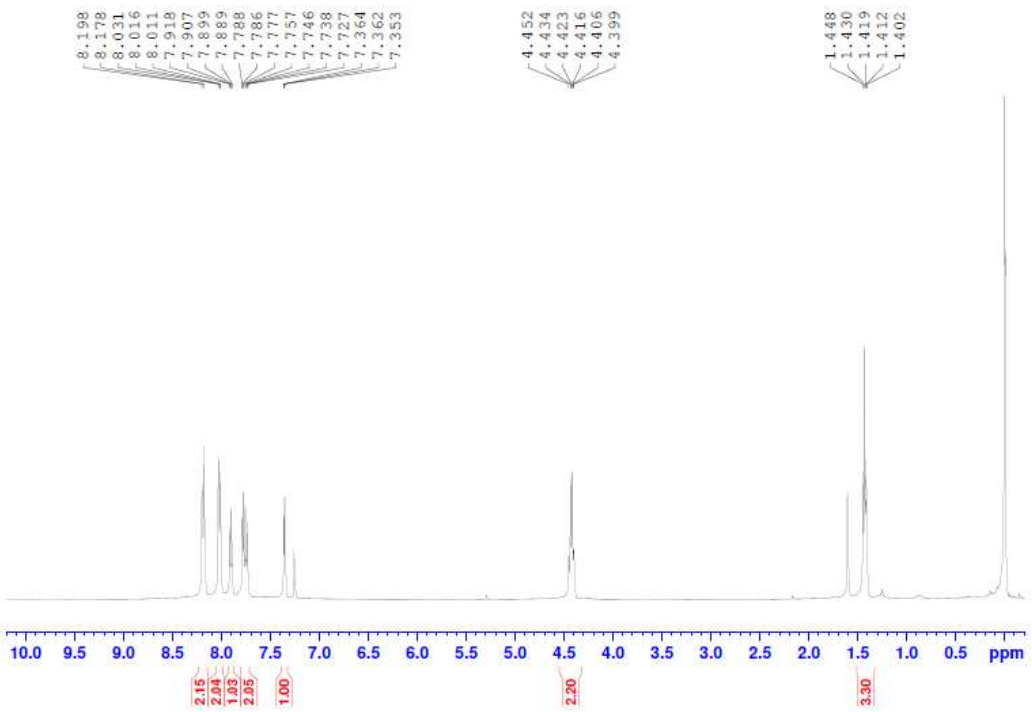

Figure S11. ^{1}H NMR spectrum of **6a** in $CDCl_3$.

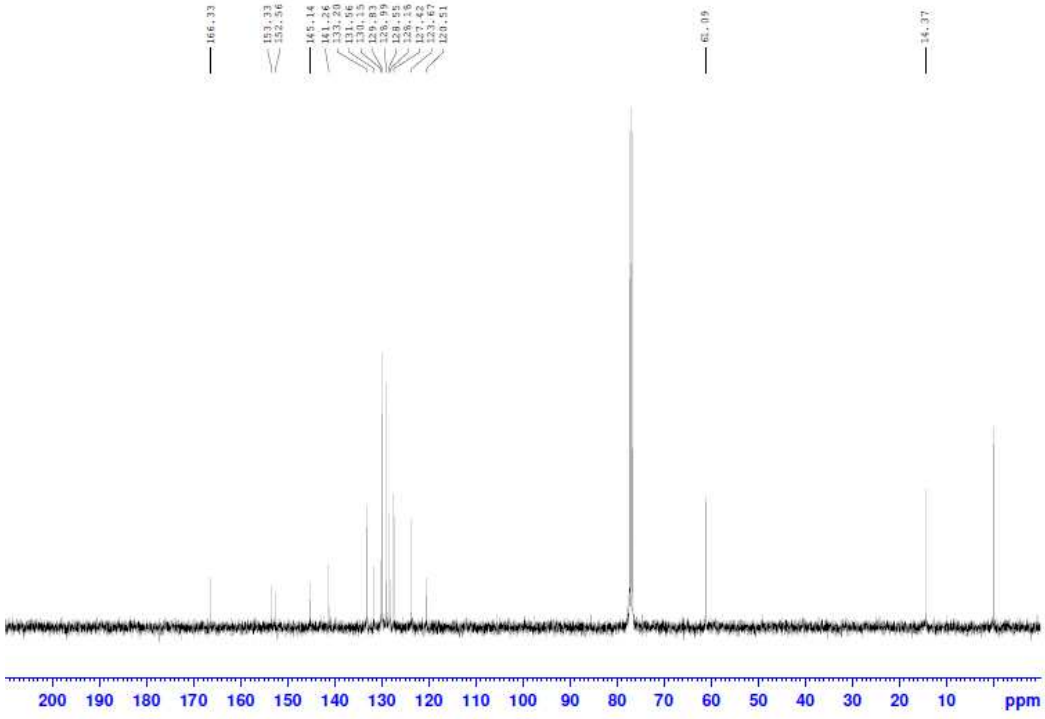

Figure S12. ^{13}C NMR spectrum of **6a** in $CDCl_3$.

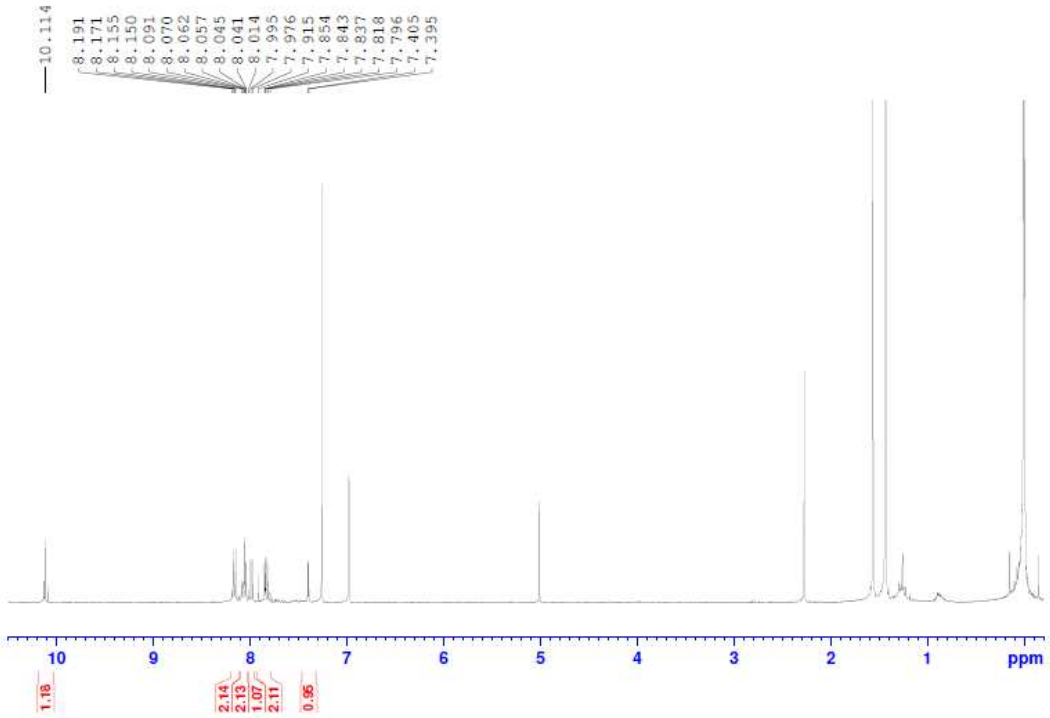

Figure S13. ^{1}H NMR spectrum of **6b** in $CDCl_3$.

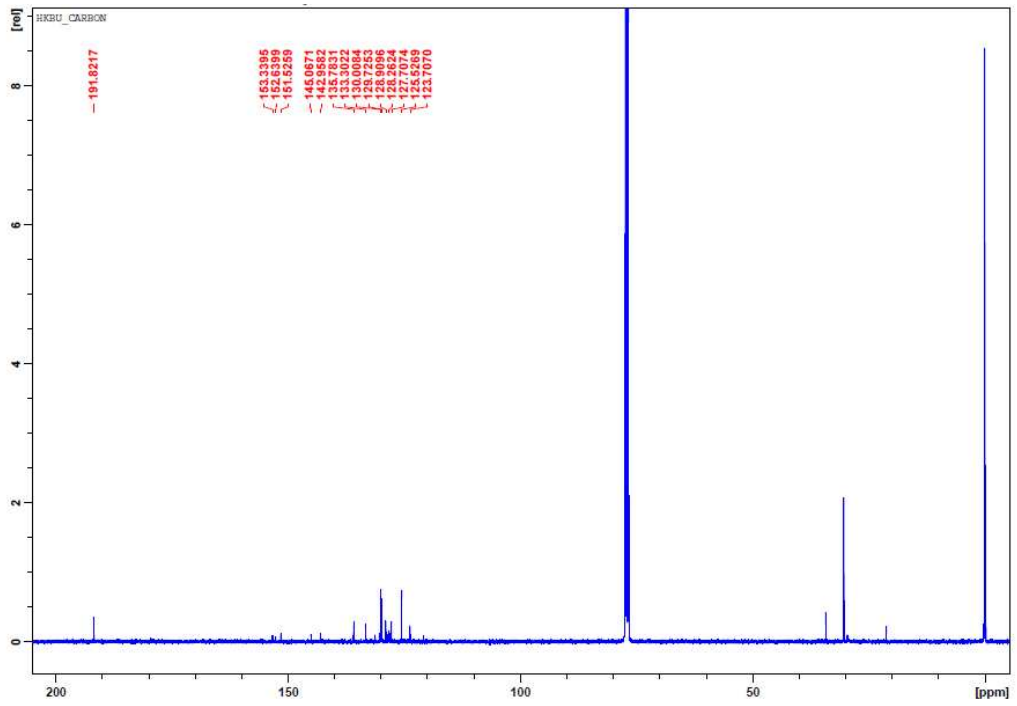

Figure S14. ^{13}C NMR spectrum of **6b** in $CDCl_3$.

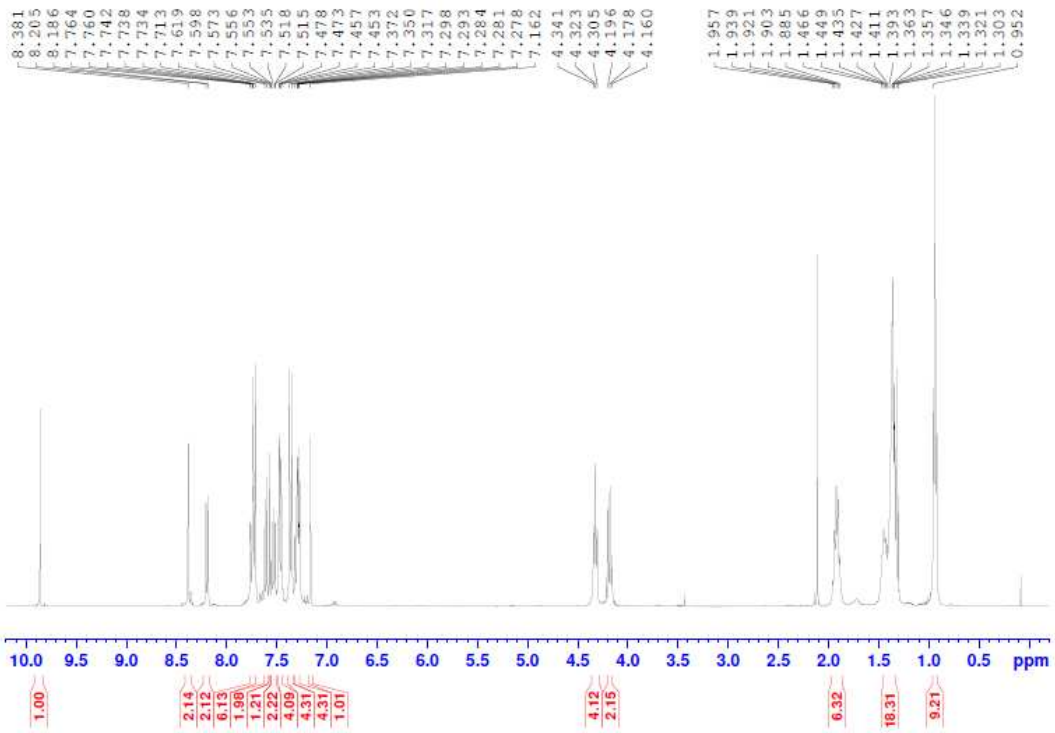

Figure S15. ^{1}H NMR spectrum of **7a** in $CDCl_3$.

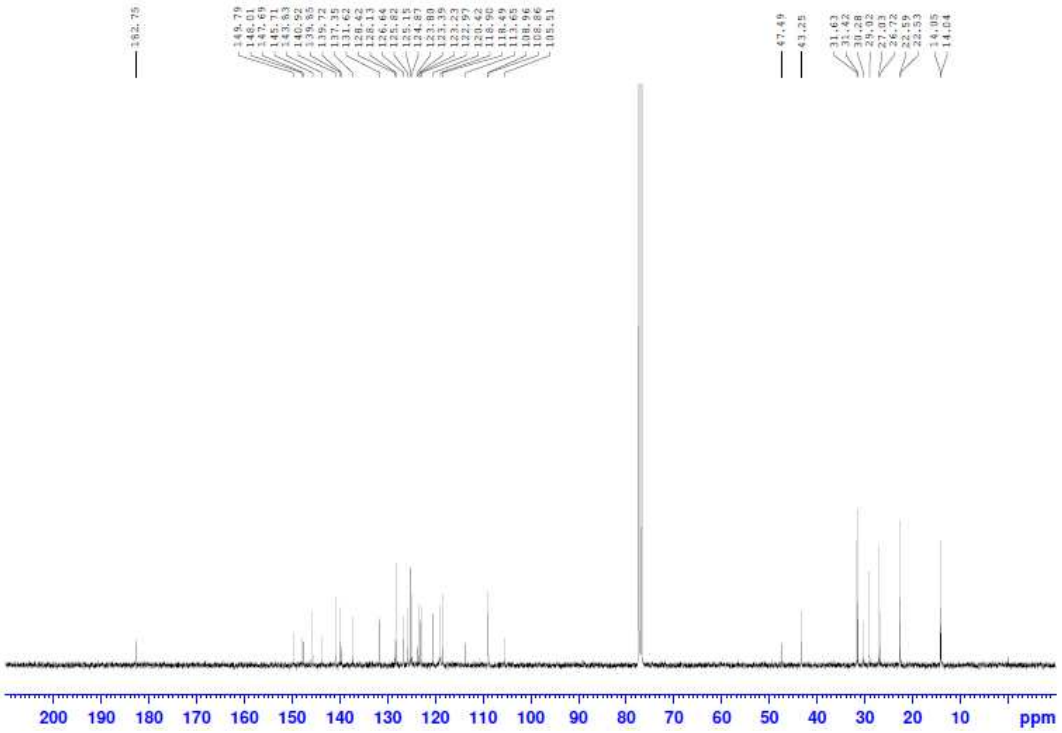

Figure S16. ^{13}C NMR spectrum of **7a** in $CDCl_3$.

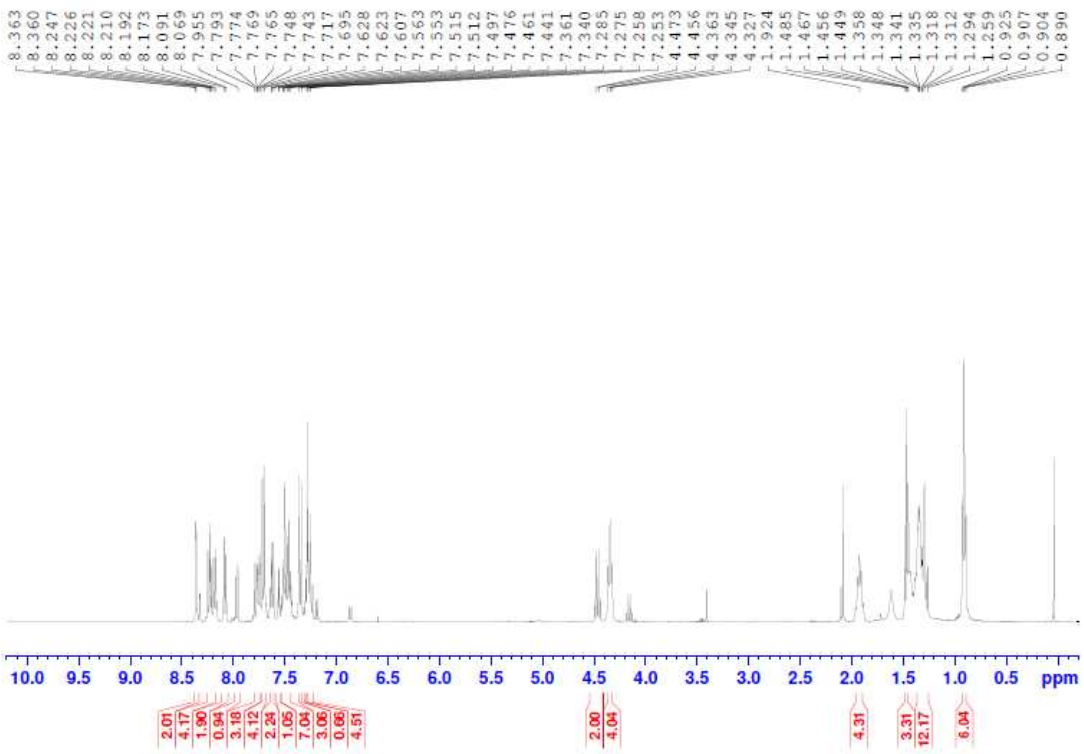

Figure S17. ^{1}H NMR spectrum of **7b** in $CDCl_3$.

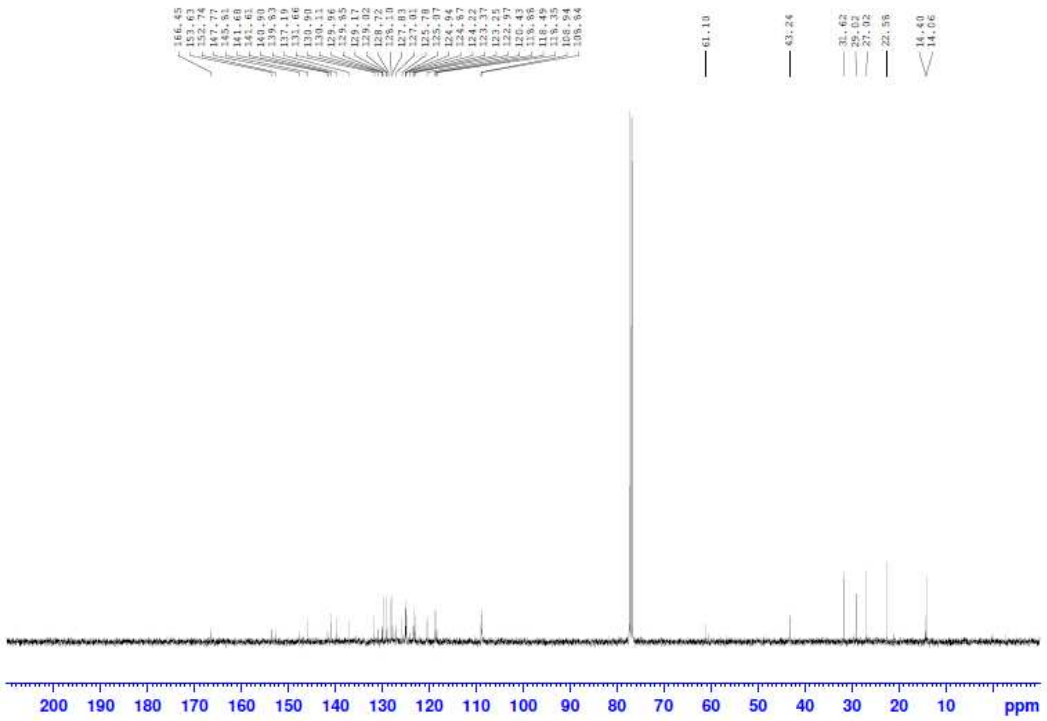

Figure S18. ^{13}C NMR spectrum of **7b** in $CDCl_3$.

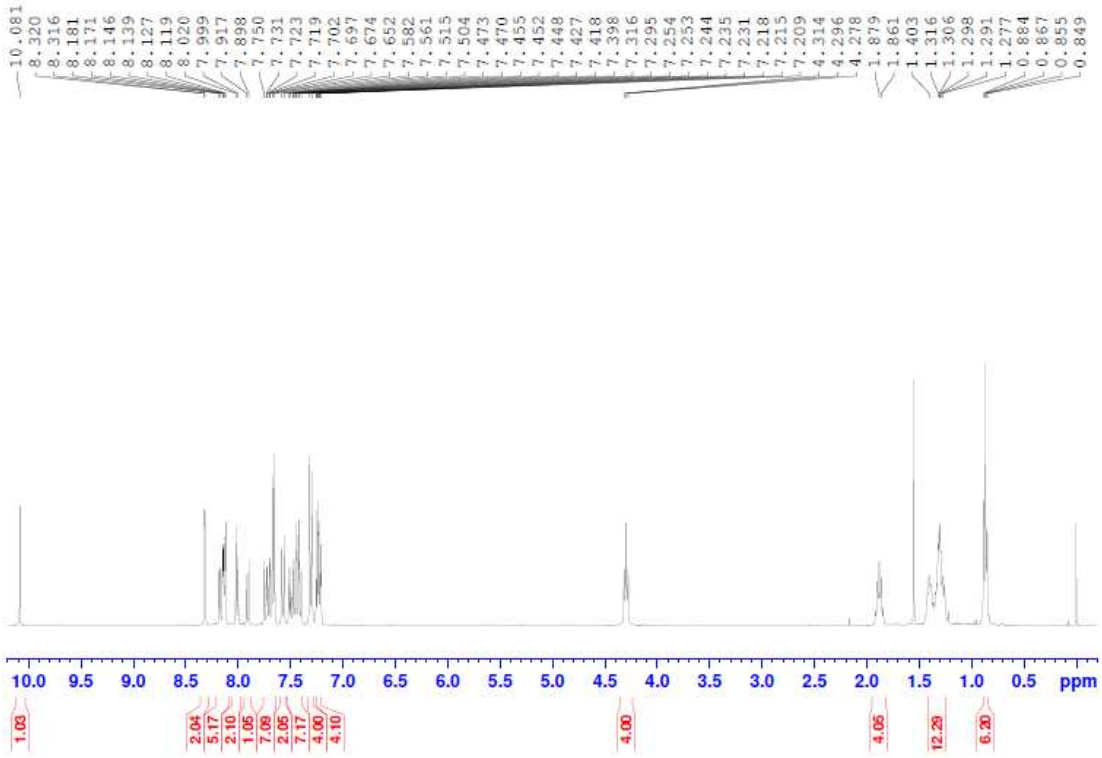

Figure S19. ^{1}H NMR spectrum of **7c** in $CDCl_3$.

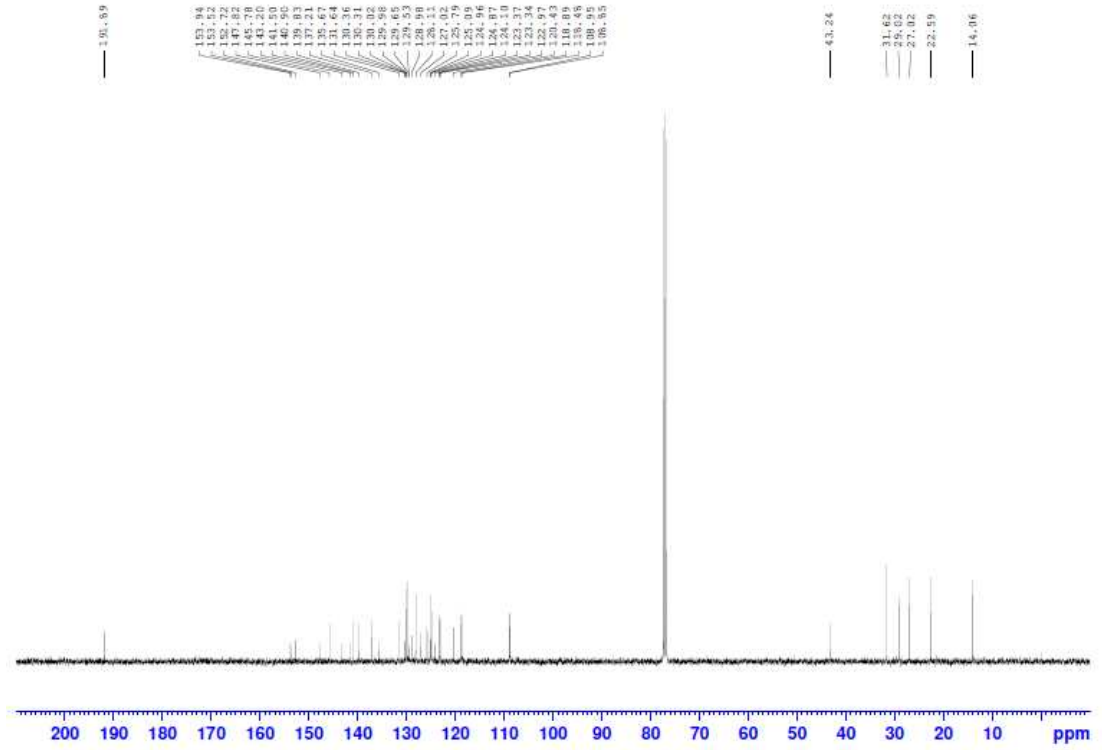

Figure S20. ^{13}C NMR spectrum of **7c** in $CDCl_3$.

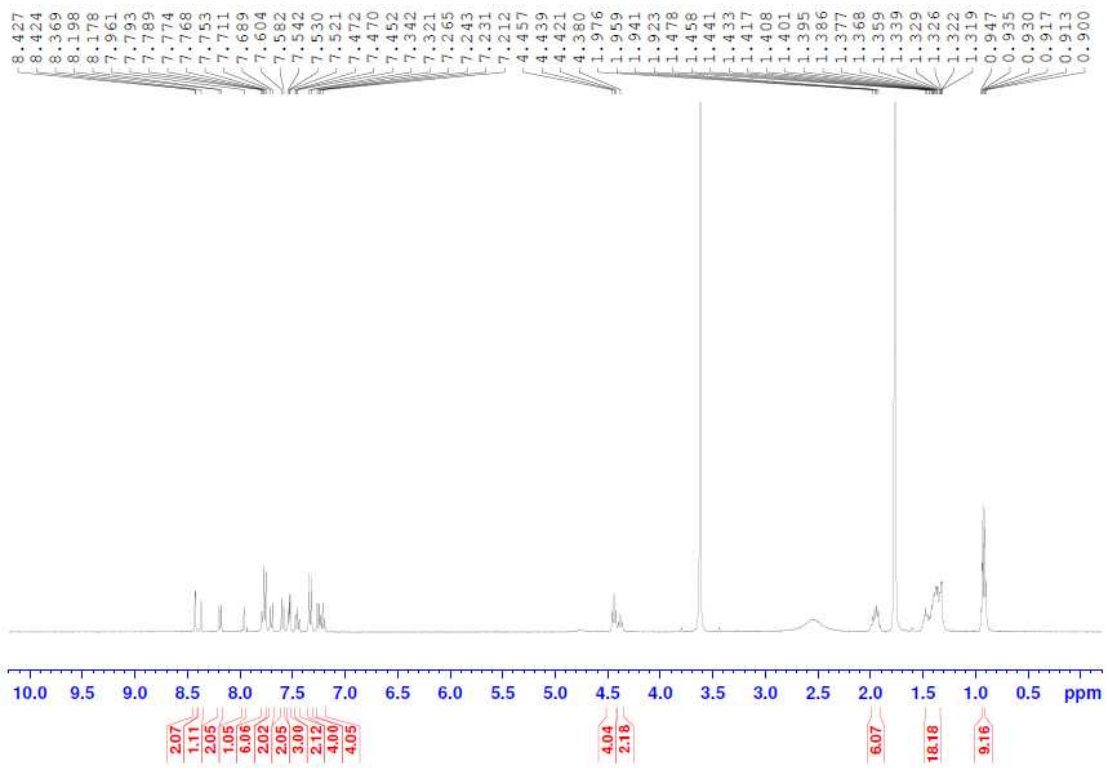

Figure S21. ^{1}H NMR spectrum of **S1** in THF-d_8.

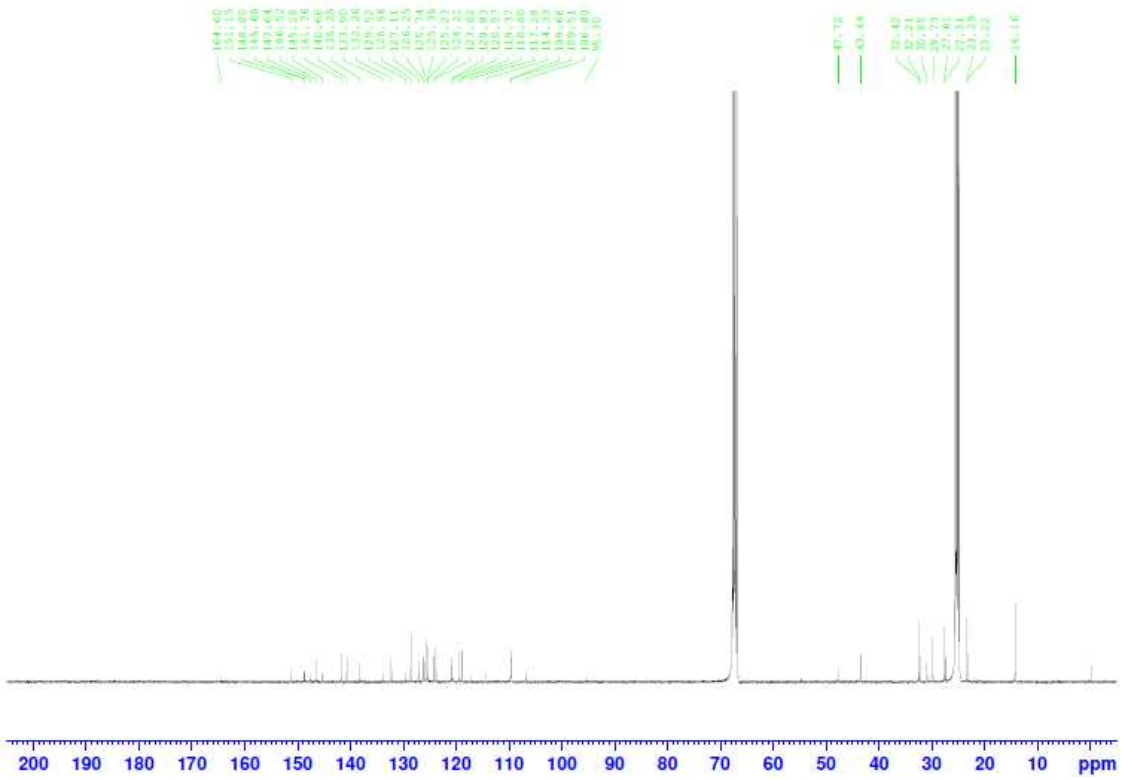

Figure S22. ^{13}C NMR spectrum of **S1** in THF-d_8.

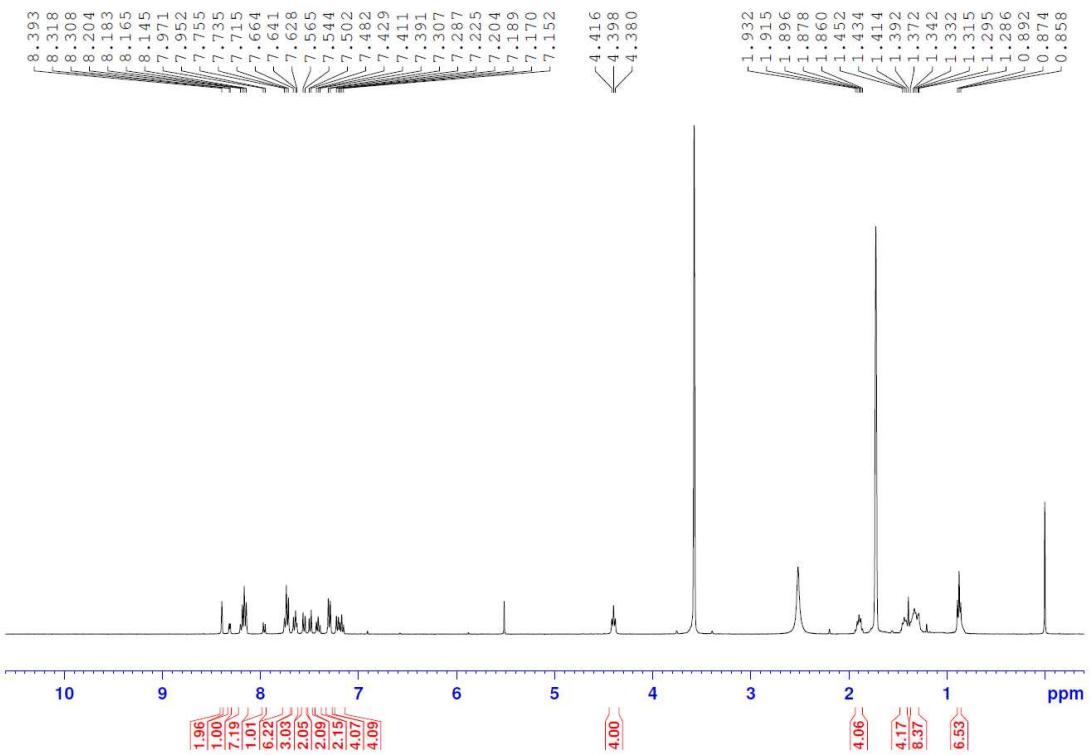

Figure S23. ^{1}H NMR spectrum of **S2** in THF-d_8.

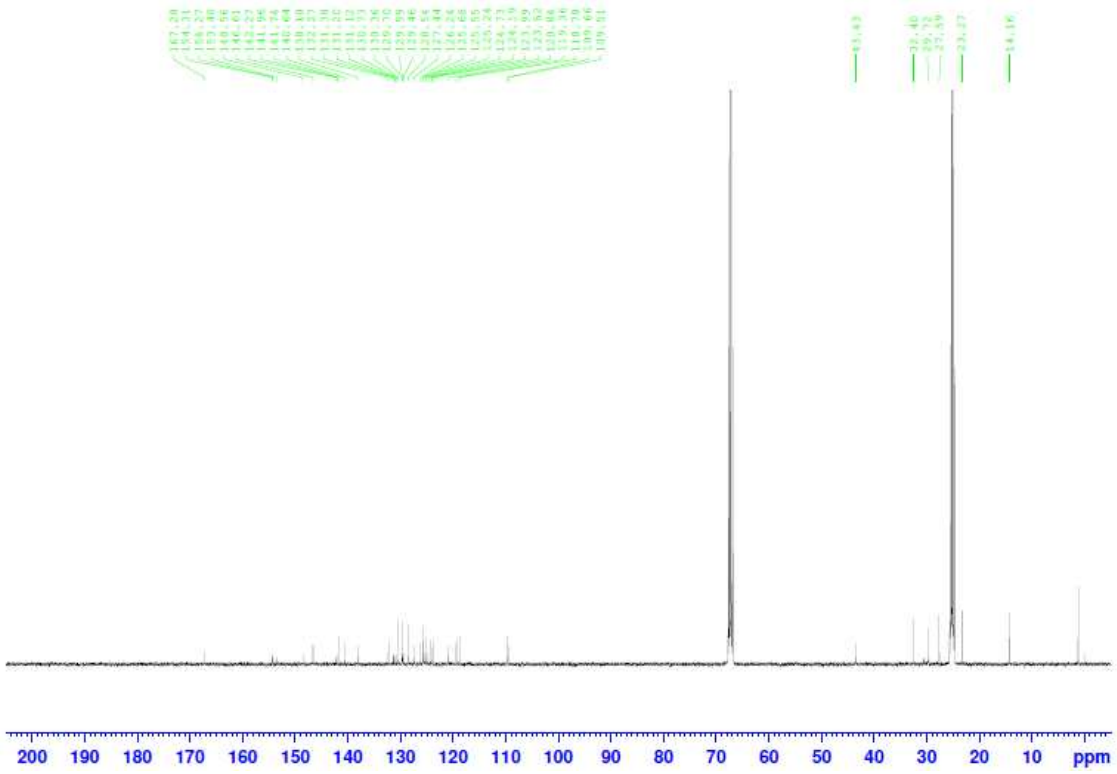

Figure S24. ^{13}C NMR spectrum of **S2** in THF-d_8.

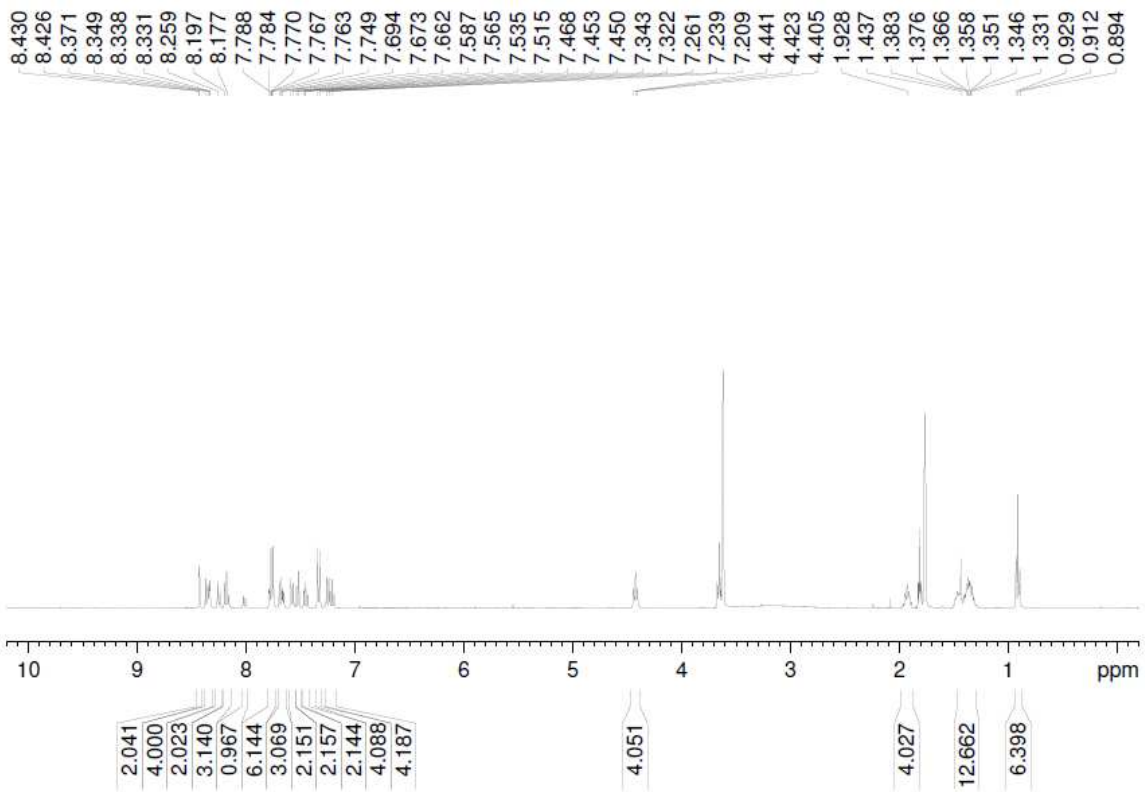

Figure S25. ^{1}H NMR spectrum of **S3** in THF-d_8.

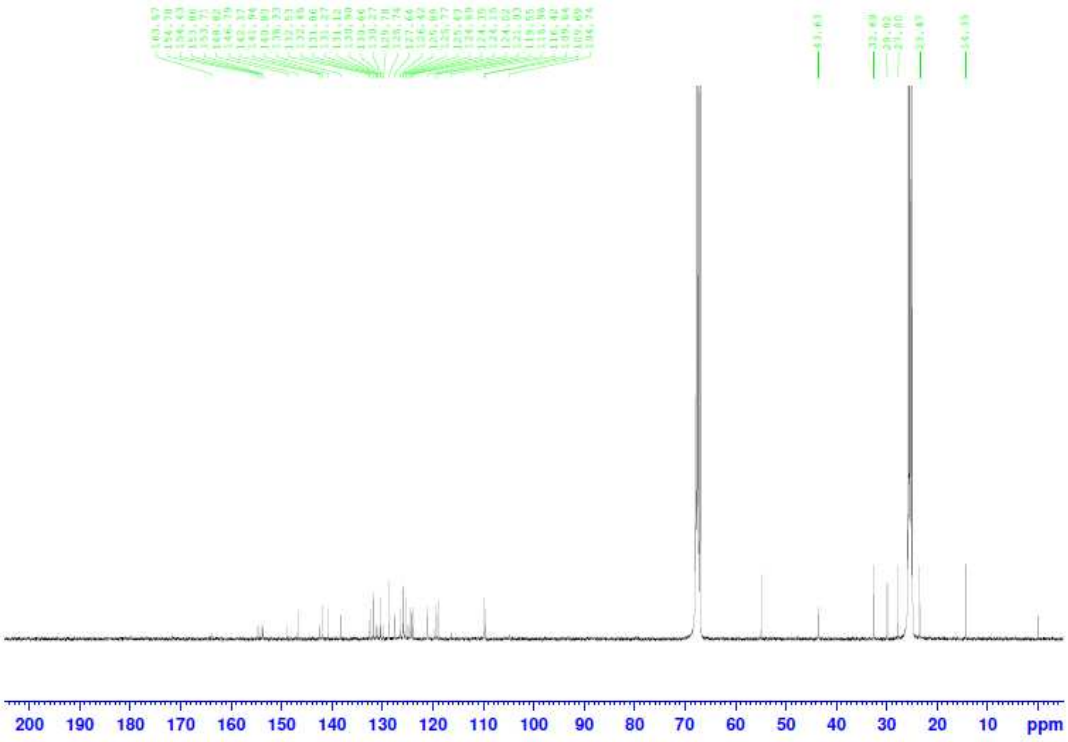

Figure S26. ^{13}C NMR spectrum of **S3** in THF-d_8.

4. Computational studies

Density functional theory (DFT) calculations and time-dependent density functional theory (TD-DFT)[4] calculations provide useful information for the nature of electronic ground states and excited states, respectively. Both DFT and TD-DFT calculations were performed by using the Gaussian 09 package.[5] The Perdew–Burke–Ernzerhof form of Generalized Gradient Approximation (GGA-PBE)[6], the B3LYP[7], hybrid functional with 20% Hatree-Fock exchange and minnesota hybrid exchange-correlation functional M06[8] with 27% Hatree-Fock exchange were used. The 6-31G(d,p) basis set was used for C, H, N, O, S, and Se. The optimized geometries for **S1**–**S3** were confirmed with all real frequencies.

For **S1**–**S3**, the electron density in HOMO is associated with the donor moiety and the π-linker, while the LUMO is localized at the electron acceptor (Figure S27). The GGA-PBE underestimates the HOMO-LUMO gap while the M06 overestimates it (Table S1). The B3LYP gives the gaps close to experimental ones. But the calculated gaps of **S1**, **S2**, and **S3** by GGA-PBE, B3LYP and M06 functionals have the same trend: the calculated gap of **S3** is smaller than that of **S1** and **S2**, in agreement with the experimental result.

The calculated absorption spectra have two broad peaks in the range of 300−650 nm and this is consistent with the experimental absorption (Figure 2(a)). The peak in the range of 450−650 nm is mainly originated from HOMO to LUMO transition for **S1**–**S3**, the charge of which is transferred from donor to acceptor (Table S2 and Figure S27). The peak in the range of 350–450 nm for **S1** and **S3** arises from the π−π* transitions among aromatic rings (Table S2, and Figure S27, S29 and S31), while the peak for **S2** is attributed to both ICT and π−π* transitions (Table S2, and Figure S27 and S30).

Table S1. The Calculated HOMO-LUMO Gap (eV) by GGA-PBE, B3LYP, and M06 functionals

	GGA-PBE	B3LYP	M06	Expt.
S1	1.24	2.19	2.60	2.04
S2	1.03	2.10	2.51	2.08
S3	0.89	1.89	2.30	1.97

Table S2. The Absorption Wavelength (nm), Oscillator Strength *f*, and Orbital Transition Contribution of Several Absorptions with High Oscillator Strength for **S1**–**S3** by M06 Functional

	Absorption (300 ~ 450 nm)		Absorption (450 ~ 650 nm)	
S1	**350.58 nm f = 0.8718**		**567.84 nm f = 1.3818**	
	HOMO -> LUMO+2	63%	HOMO -> LUMO	95%
	HOMO -> LUMO+4	28%		
S2	**352.55 nm f = 0.9072**		**596.83 nm f = 0.7872**	
	HOMO -> LUMO+3	60%	HOMO-2 -> LUMO	7%
	HOMO-> LUMO+5	32%	HOMO -> LUMO	91%
	401.32 nm f = 0.8878			
	HOMO-2 -> LUMO+1	6%		
	HOMO -> LUMO+1	69%		
	HOMO -> LUMO+2	18%		
S3	**352.09 nm f = 0.8918**		**644.59 nm f = 0.9047**	
	HOMO -> LUMO+3	62%	HOMO-2 -> LUMO	5%
	HOMO -> LUMO+5	30%	HOMO -> LUMO	91%

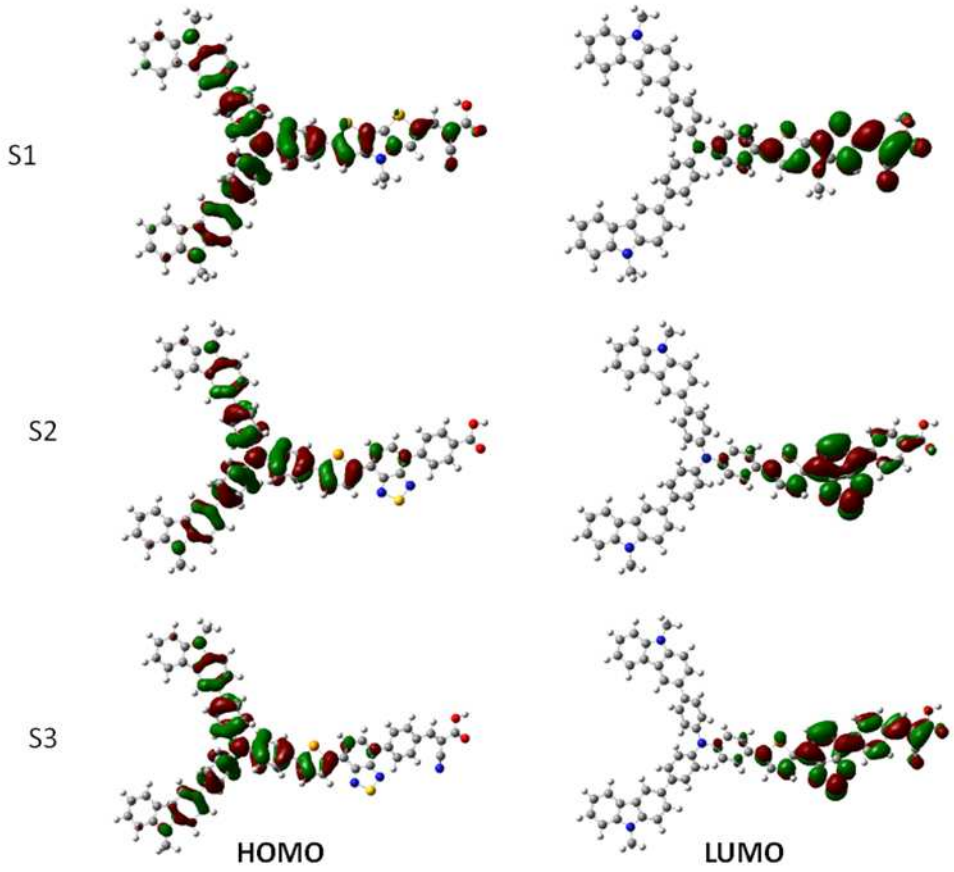

Figure S27. The HOMO and LUMO of **S1**–**S3** by M06 functional. The GGA-PBE and B3LYP functional give similar pictures.

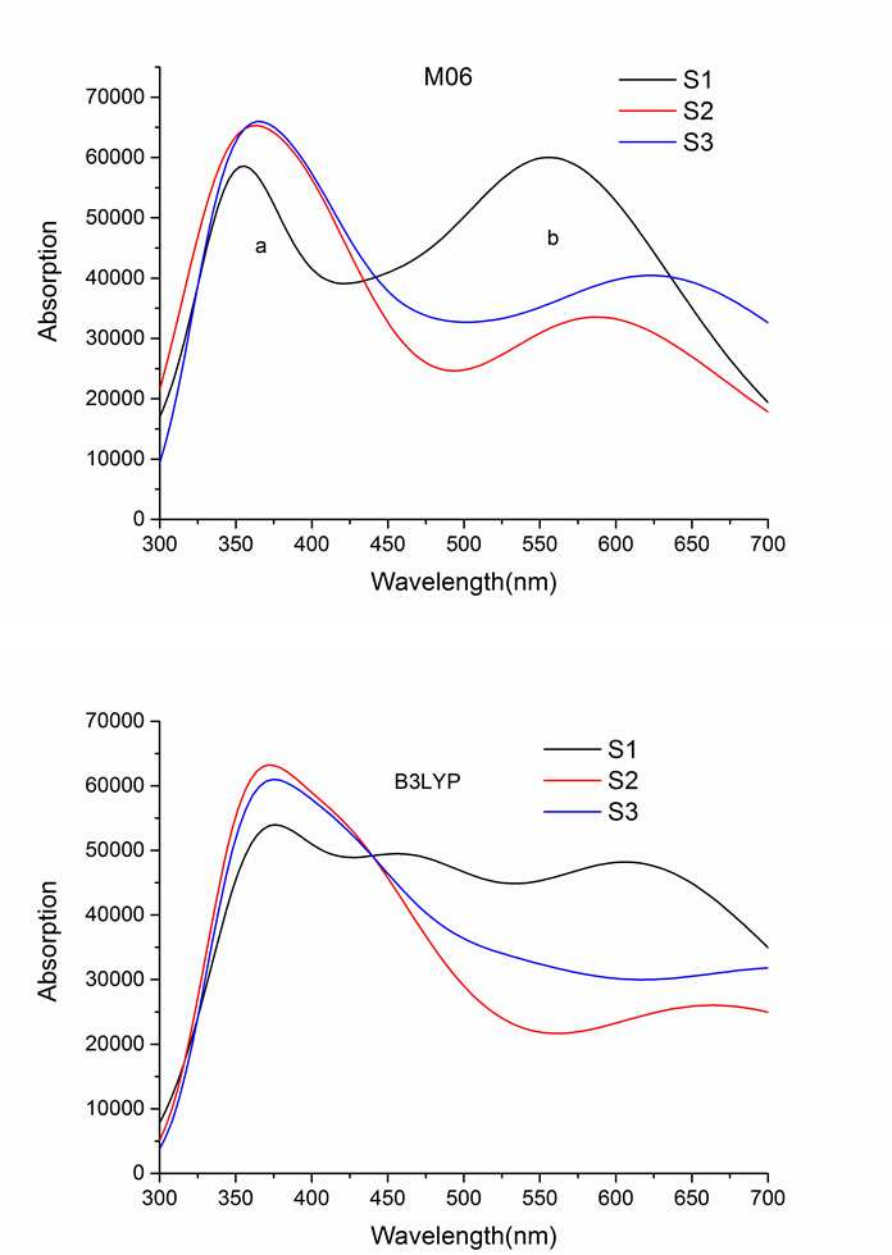

Figure S28. The calculated absorption spectra for **S1**–**S3** by M06 and B3LYP functionals.

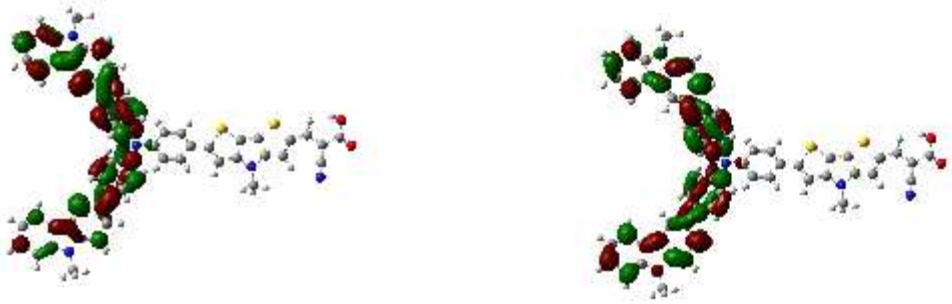

LUMO+2 LUMO+4

Figure S29. The frontier orbitals of **S1** by M06 functional. The GGA-PBE and B3LYP functional give similar pictures.

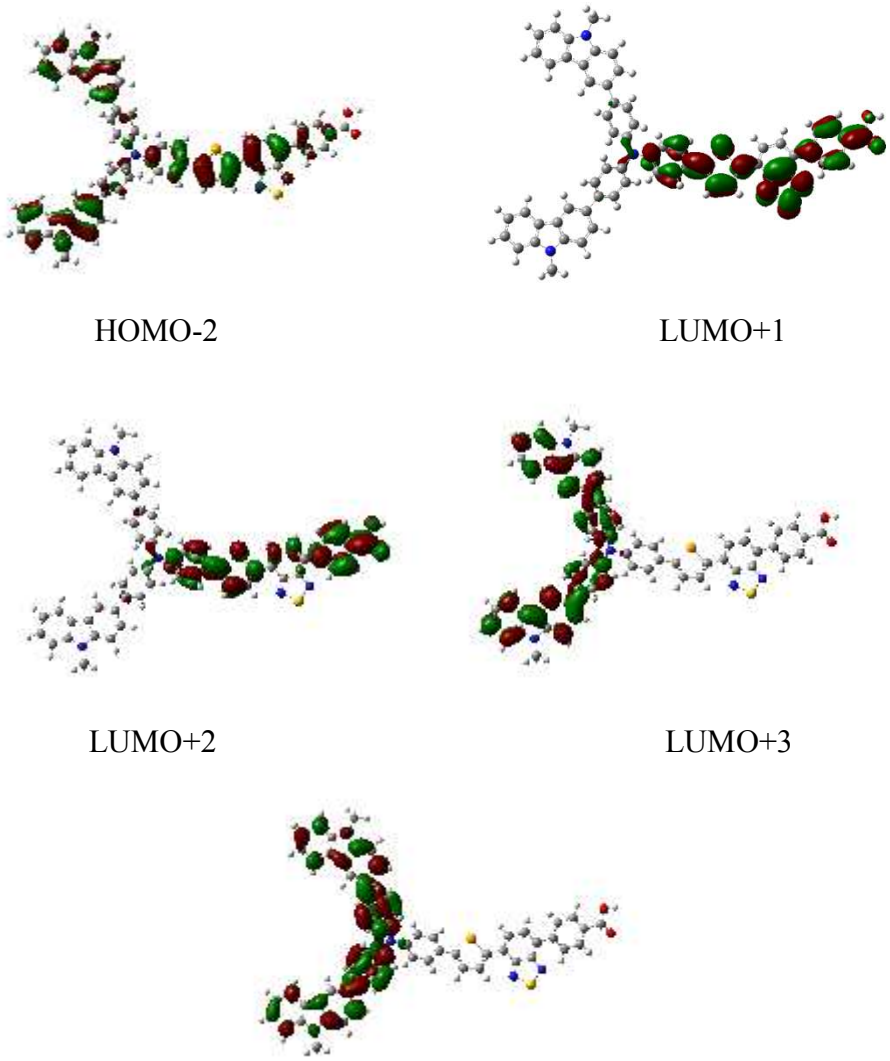

Figure S30. The frontier orbitals of **S2** by M06 functional. The GGA-PBE and B3LYP functional give similar pictures.

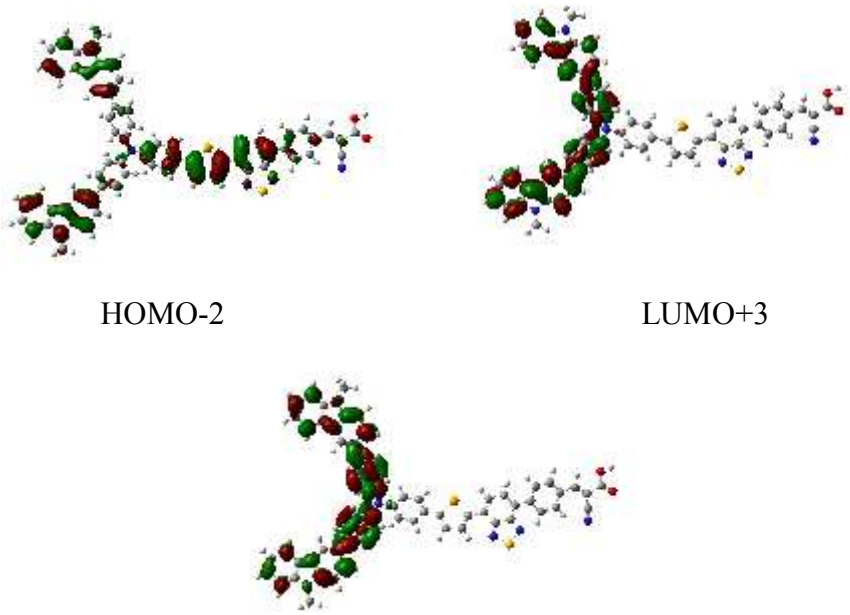

Figure S31. The frontier orbitals of **S3** by M06 functional. The GGA-PBE and B3LYP functional give similar pictures.

5. Cyclic voltammograms

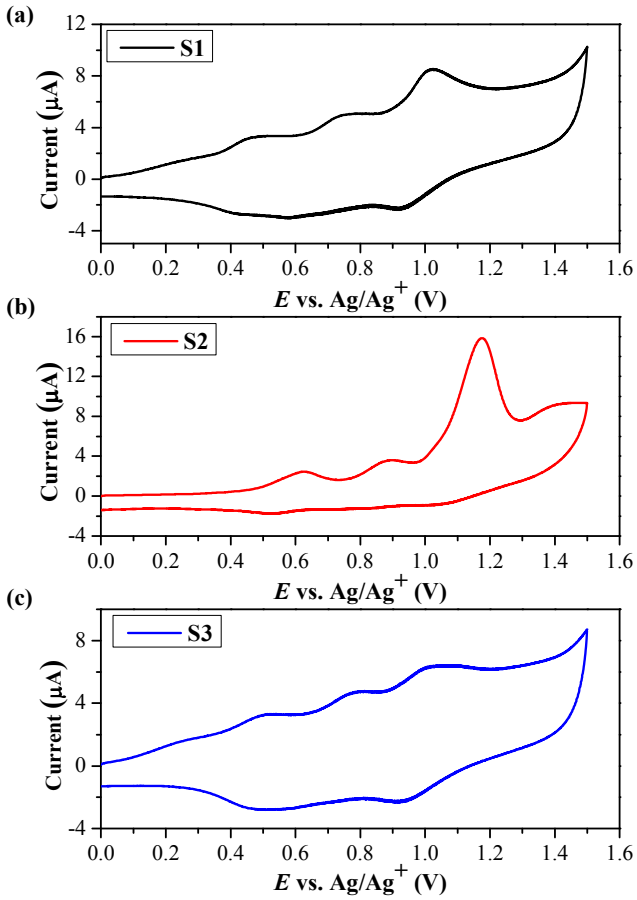

Figure S32. Cyclic voltammograms of photosensitizers **S1**–**S3** in CH_2Cl_2 solution (1×10^{-4} M).

Table S3. Electrochemical Data and Energy Levels of **S1**–**S3**

Dye	E_{ox} [a] /V	E_{HOMO} [b] /eV	E_{0-0} [c] /eV	E_{ox*} [d] /V	E_{LUMO} [e] /eV
S1	0.31	–5.02	2.04	–1.73	–2.98
S2	0.42	–5.13	2.08	–1.66	–3.05
S3	0.30	–5.01	1.97	–1.67	–3.04

[a]Onset oxidation potentials were measured by cyclic voltammetry in dry CH_2Cl_2 solution containing 0.1 M of $[NBu_4][PF_6]$ as the supporting electrolyte (vs. Ag/Ag^+ reference electrode). Under these conditions, the reversible oxidation of ferrocene was $E_{1/2} = 0.09$ V. [b]Calculated from $-(E_{ox} + 4.71)$, as the E_{HOMO} of ferrocene is equal to –4.80 eV vs. to vacuum level. [c]E_{0-0} was determined from the onset of absorption spectrum. [d]$E_{ox*} = E_{ox} - E_{0-0}$. [e] $E_{LUMO} = E_{HOMO} + E_{0-0}$.

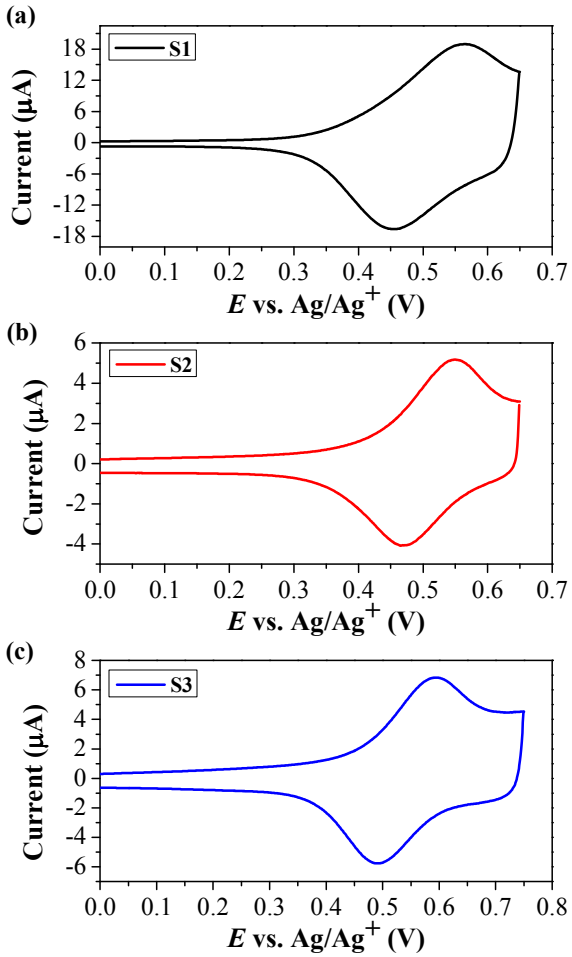

Figure S33. Cyclic voltammograms of photosensitizers **S1**–**S3** in CH_2Cl_2 solution (5×10^{-4} M). The scan range is limited for the first oxidation wave for each PS. All the oxidation waves are reversible, since the anodic current is equal to the cathodic current and the peak potential difference is similar to that of ferrocenium/ferrocene couple for each PS.

6. Photovoltaic performances and EIS Nyquist plots of DSSCs

Table S4. Photovoltaic Performances of DSSCs with Photosensitizers **S1**–**S3** under AM 1.5 Sunlight Illumination and the Parameters Obtained by Fitting the EIS Spectra of the DSSCs

Dye	J_{sc} /mA cm^{-2}	V_{oc} /V	FF	PCE /%	R_{rec} /Ω
S1	14.23	0.68	0.679	6.59	181.80
S2	13.50	0.68	0.673	6.21	182.77
S3	12.61	0.65	0.669	5.55	178.85

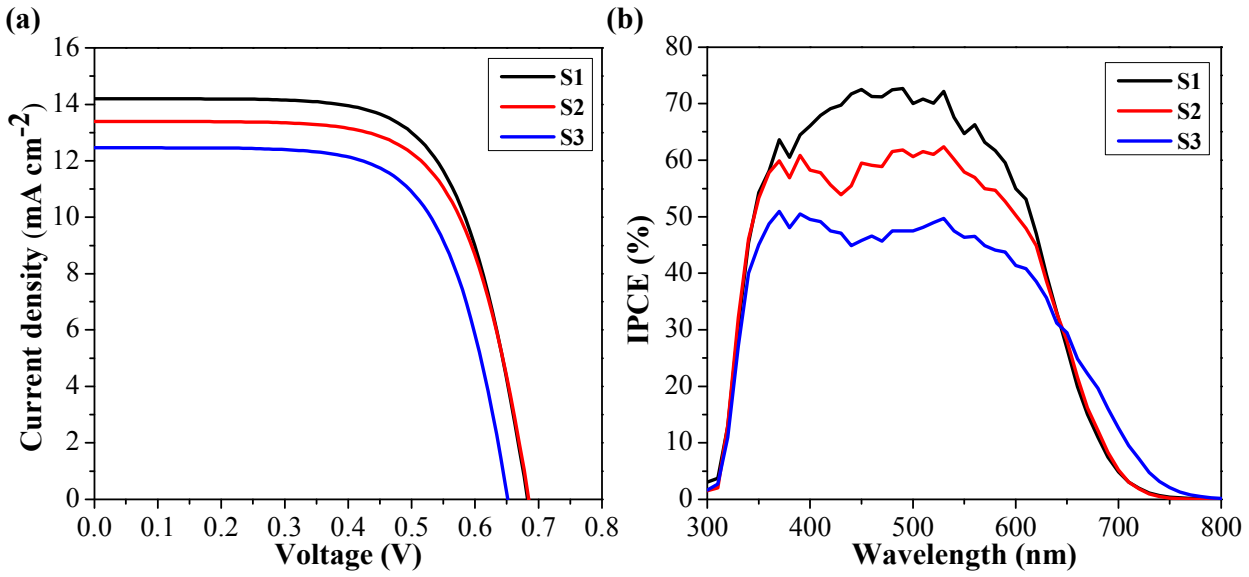

Figure S34. (a) Photocurrent density–voltage (*J*–*V*) plots obtained with **S1**–**S3**. (b) Incident photon–to–current efficiency (IPCE) curves obtained with **S1**–**S3**.

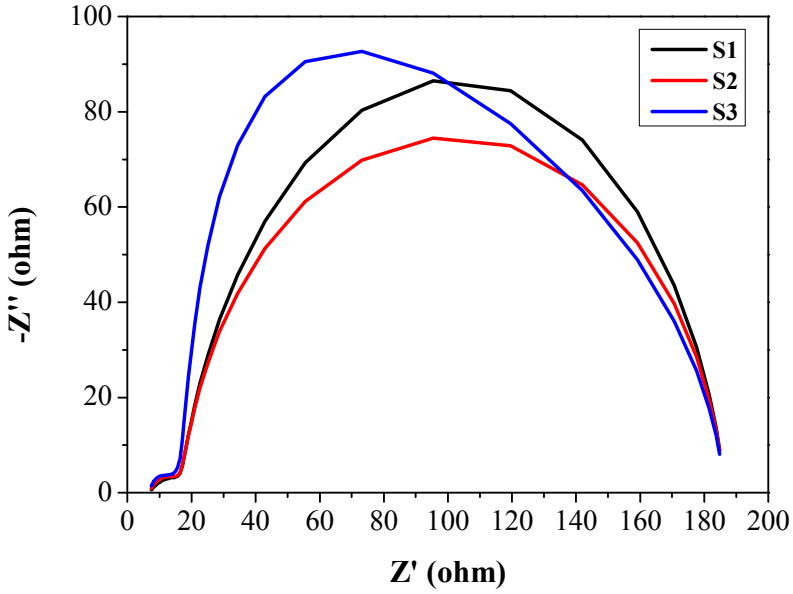

Figure S35. EIS Nyquist plots for DSSCs based on **S1**−**S3** under darkness.

7. UV/vis absorption spectra of PSs before and after dye adsorption

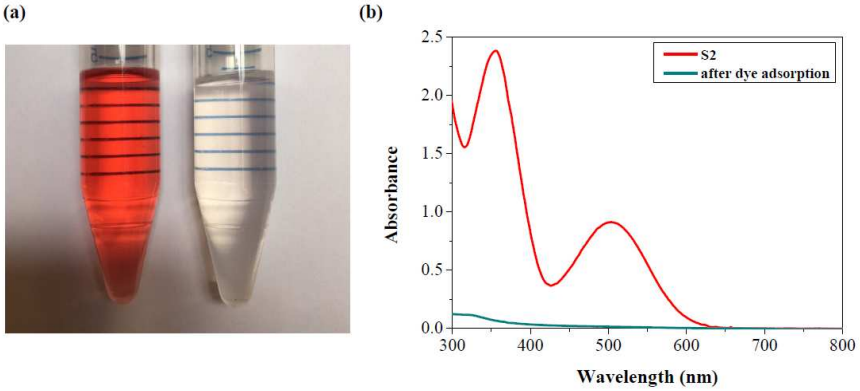

Figure S36. (a) Image of 50 μM photosensitizer **S2** solution in CH_2Cl_2 before (left) and after (right) dye adsorption on platinized TiO_2. (b) UV/vis absorption spectra of **S2** in dichloromethane solution before and after dye adsorption.

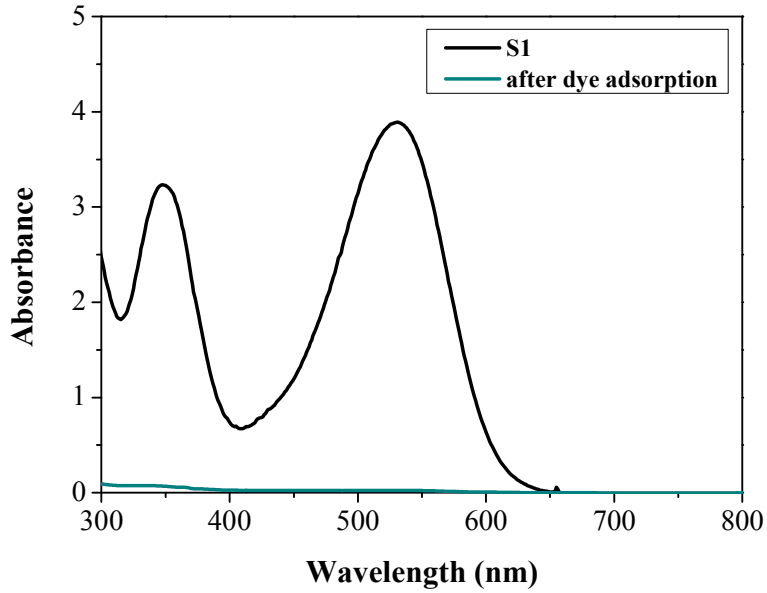

Figure S37. UV/vis absorption spectra of **S1** in CH_2Cl_2 at 293K before and after dye adsorption.

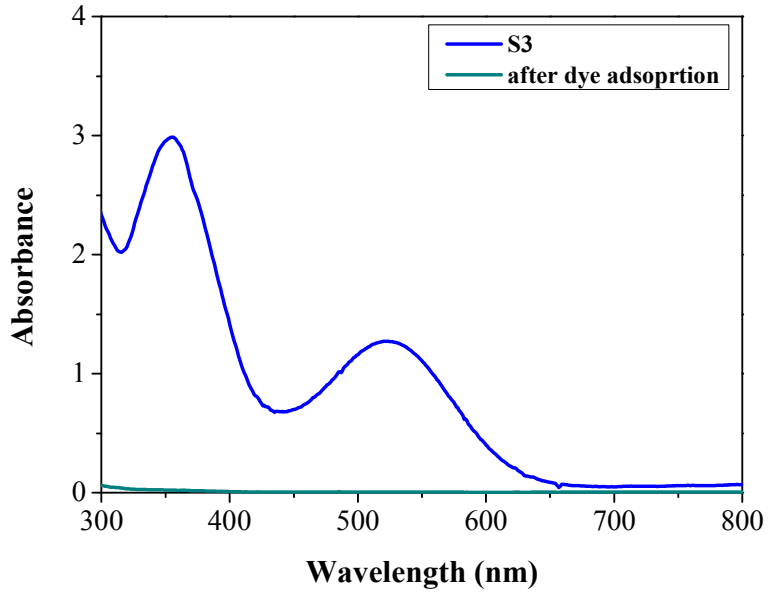

Figure S38. UV/vis absorption spectra of **S3** in CH_2Cl_2 at 293K before and after dye adsorption.

8. Calibration plot for H_2 measurement

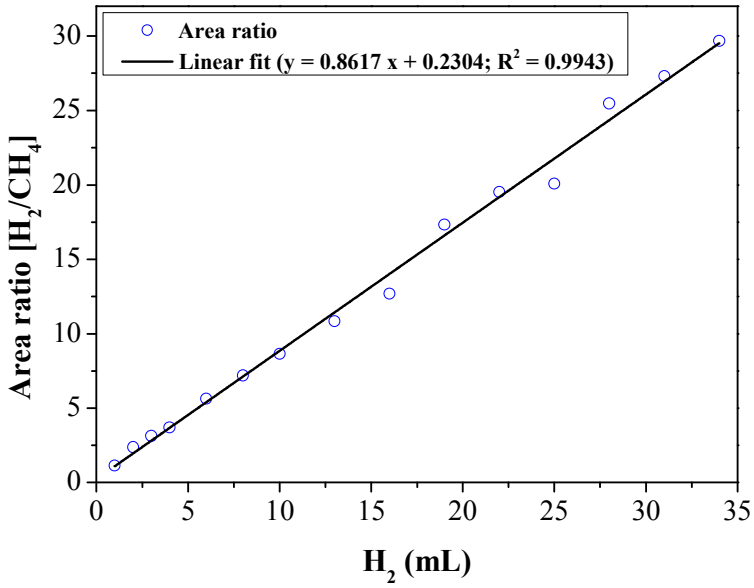

Figure S39. Calibration plot of the signal ratio (H_2/CH_4) vs. amount of H_2 obtained from GC analysis.

9. Illustration of photocatalytic reaction mixture with S1 before and after the irradiation

Figure S40. Image of 5 mL 0.5 M ascorbic acid in water at pH 4.0 with 20 mg of **S1**-TiO_2-Pt before (a) and after (b) 48 hours green LED irradiation. (c) Image of the corresponding reaction mixture after centrifugation at 3500 rpm for five minutes.

10. Performance of triarylamine analogue PSs, and some Ru(II), Ir(III) and Pt(II) complex-based PSs in light-driven H_2 generation

Table S5. Performance of Ru(II), Ir(III) and Pt(II) Complexes in Some Representative Photocatalytic H_2 Generation Studies[a]

no.	reference	metal	PS	TON/ activity	Time
1	*Energy Environ. Sci.* **2014**, *7*, 1477–1488	Ru(II)	$[Ru(bpy)_3]Cl_2$	375 μmol of H_2	15 h
2	*Chem. Commun.* **2010**, *46*, 7551–7553	Ir(III)	$[Ir(F\text{-}mppy)_2(mVbpy)]PF_6$	TON > 8500	48 h
3	*J. Am. Chem. Soc.* **2011**, *133*, 11819–11821	Ir(III)	$[Ir(fmppy)_2(qpy)]PF_6$	TON ~ 6000	40 h
4	*Proc. Natl. Acad. Sci. U. S. A.* **2015**, *112*, E3987–E399	Pt(II)	4(byP), R= $PO(OEt)_2$	TON = 15400	60 h

[a]Only the best performance in each study is reported.

Table S6. Performance of Triarylamine Analogue PSs in Photocatalytic H_2 Production Studies[a]

no.	reference	PS	TON/ activity	Time
1	*Org. Lett.* **2010**, *12*, 460–463	DEO2	TON = 800[b]	5 h
2	*Appl. Catal., B* **2012**, *121–122*, 206–213	D3	111 μmol of H_2	1.5 h
3	*Chem. Eur. J.* ***2012****, 18, 15368–15381*	MOD	TON = 17	4 h
4	*ChemSusChem* **2014**, *7*, 2879–2888	AQ	30 μmol of H_2	10 h
5	*Int. J. Hydrogen Energy* **2015**, *40*, 9069–9079	DN-F05	TON = 1864	6 h

[a]Only the best performance in each study is reported. [b]Estimated from a review article.[9]

References

(1) Ito, S.; Murakami, T. N.; Comte, P.; Liska, P.; Grätzel, C.; Nazeeruddin, M. K.; Grätzel, M. *Thin Solid Films* **2008**, *516*, 4613–4619.

(2) Liu, B.; Zhu, W.; Wang, Y.; Wu, W.; Li, X.; Chen, B.; Long, Y.-T.; Xie, Y. *J. Mater. Chem.* **2012**, *22*, 7434–7444.

(3) Natali, M. *ACS Catal.* **2017**, 1330–1339.

(4) Marques, M. A. L.; Gross, E. K. U. *Annu. Rev. Phys. Chem.* **2004**, *55*, 427–455.

(5) Frisch, M. J.; Trucks, G. W.; Schlegel, H. B.; Scuseria, G. E.; Robb, M. A.; Cheeseman, J. R.; Scalmani, G.; Barone, V.; Mennucci, B.; Petersson, G. A.; Nakatsuji, H.; Caricato, M.; Li, X.; Hratchian, H. P.; Izmaylov, A. F.; Bloino, J.; Zheng, G.; Sonnenberg, J. L.; Hada, M.; Ehara, M.; Toyota, K.; Fukuda, R.; Hasegawa, J.; Ishida, M.; Nakajima, T.; Honda, Y.; Kitao, O.; Nakai, H.; Vreven, T.; Montgomery Jr., J. A.; Peralta, J. E.; Ogliaro, F.; Bearpark, M. J.; Heyd, J.; Brothers, E. N.; Kudin, K. N.; Staroverov, V. N.; Kobayashi, R.; Normand, J.; Raghavachari, K.; Rendell, A. P.; Burant, J. C.; Iyengar, S. S.; Tomasi, J.; Cossi, M.; Rega, N.; Millam, N. J.; Klene, M.; Knox, J. E.; Cross, J. B.; Bakken, V.; Adamo, C.; Jaramillo, J.; Gomperts, R.; Stratmann, R. E.; Yazyev, O.; Austin, A. J.; Cammi, R.; Pomelli, C.; Ochterski, J. W.; Martin, R. L.; Morokuma, K.; Zakrzewski, V. G.; Voth, G. A.; Salvador, P.; Dannenberg, J. J.; Dapprich, S.; Daniels, A. D.; Farkas, Ö.; Foresman, J. B.; Ortiz, J. V.; Cioslowski, J.; Fox, D. J. *Gaussian 09, Revision E.01*, Gaussian, Inc.: Wallingford CT, 2009.

(6) Perdew, J. P.; Burke, K.; Ernzerhof, M. *Phys. Rev. Lett.* **1996**, *77*, 3865–3868.

(7) (a) Becke, A. D. *Phys. Rev. A* **1988**, *38*, 3098–3100; (b) Lee, C.; Yang, W.; Parr, R. G. *Phys. Rev. B* **1988**, *37*, 785–789; (c) Stephens, P. J.; Devlin, F. J.; Chabalowski, C. F.; Frisch, M. J. *J. Phys. Chem.* **1994**, *98*, 11623–11627.

(8) Zhao, Y.; Truhlar, D. G. *Theor. Chem. Acc.* **2008**, *120*, 215–241.

(9) Cecconi, B.; Manfredi, N.; Montini, T.; Fornasiero, P.; Abbotto, A. *Eur. J. Org. Chem.* **2016**, *2016*, 5194–5215.